

### Ⅲ. 研究成果の刊行に関する一覧表

研究成果の刊行に関する一覧表レイアウト

書籍

著者氏名	論文タイトル名	書籍全体の編集者名	書籍名	出版社名	出版地	出版年	ページ
		<u>Masaki Otagiri</u> (全体編集)	HUMAN SERUM ALBUMIN	Sojo University Publishing Center	Japan	2013	1-510
Taguchi K, Chuang VT, Maruyama T, <u>Otagiri M.</u>	Molecular Aspects of Human Alpha-1 Acid Glycoprotein; Structure and Function	Sabina Janciauskiene	ACUTE PHASE PROTEINS	INTECH	Croatia	2013	137-162

雑誌

発表者氏名	論文タイトル名	発表誌名	巻号	ページ	出版年
Taguchi K, Jono H, Kugimiya-Taguchi T, Nagao S, Su Y, Yamasaki K, Mizuguchi M, Maruyama T, Ando Y, <u>Otagiri M.</u>	Effect of albumin on transthyretin and amyloidogenic transthyretin Val30Met disposition and tissue deposition in familial amyloidotic polyneuropathy.	<i>Life Sci.</i>	93(25-26)	1017-1022	2013
Yamasaki K, Chuang VT, Maruyama T, <u>Otagiri M.</u>	Albumin-drug interaction and its clinical implication.	<i>Biochim Biophys Acta.</i>	1830(12)	5435-5443	2013
Anraku M, Chuang VT, Maruyama T, <u>Otagiri M.</u>	Redox properties of serum albumin.	<i>Biochim Biophys Acta.</i>	1830(12)	5465-5472	2013
Tanaka R, Watanabe H, Kodama A, Chuang VT, Ishima Y, Hamasaki K, Tanaka K, Mizushima T, <u>Otagiri M.</u> , Maruyama T.	Long-acting human serum albumin-thioredoxin fusion protein suppresses bleomycin-induced pulmonary fibrosis progression.	<i>J Pharmacol Exp Ther.</i>	345(2)	271-283	2013
Taguchi K, Ujihira H, Ogaki S, Watanabe H, Fujiyama A, Doi M, Okamura Y, Takeoka S, Ikeda Y, Handa M, <u>Otagiri M.</u> , Maruyama T.	Pharmacokinetic study of the structural components of adenosine diphosphate-encapsulated liposomes coated with fibrinogen $\gamma$ -chain dodecapeptide as a synthetic platelet substitute.	<i>Drug Metab Dispos.</i>	41(8)	1584-1591	2013
新保卓郎	診療ガイドラインの社会的意義と問題点 3) ガイドライン作成の社会的意義と評価および法的側面：信頼されるガイドラインへ	日内会誌	102	2307-2312	2013

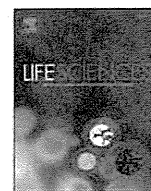
Shen H, Yamashita A, Nakakoshi M, Yokoe H, Sudo M, Kasai H, Tanaka T, Fujimoto Y, Ikeda M, Kato N, Sakamoto N, Shindo H, Maekawa S, <u>Enomoto N</u> , Tsubuki M, Moriishi K.	Inhibitory effects of caffeic Acid phenethyl ester derivatives on replication of hepatitis C virus.	<i>PLoS One.</i>	17;8(12)	e82299.	2013
Maekawa S, <u>Enomoto N</u> .	Once-daily simeprevir in combination with pegylated-interferon and ribavirin: a new horizon in the era of direct-acting antiviral agent therapy for chronic hepatitis C.	<i>J Gastroenterol.</i>	Jan;49(1)	163-4.	2014
Morisaka H, Motosugi U, Ichikawa S, Sano K, Ichikawa T, <u>Enomoto N</u> .	Association of splenic MR elastographic findings with gastroesophageal varices in patients with chronic liver disease.	<i>J Magn Reson Imaging.</i>	Nov 14.	ePub	2013
Tsuchiya K, Asahina Y, Matsuda S, Muraoka M, Nakata T, Suzuki Y, Tamaki N, Yasui Y, Suzuki S, Hosokawa T, Nishimura T, Ueda K, Kuzuya T, Nakanishi H, Itakura J, Takahashi Y, Kurosaki M, <u>Enomoto N</u> , Izumi N.	Changes in plasma vascular endothelial growth factor at 8 weeks after sorafenib administration as predictors of survival for advanced hepatocellular carcinoma.	<i>Cancer.</i>	15;120(2)	229-37.	2013
Miura M, Maekawa S, Takano S, Komatsu N, Tatsumi A, Asakawa Y, Shindo K, Amemiya F, Nakayama Y, Inoue T, Sakamoto M, Yamashita A, Moriishi K, <u>Enomoto N</u> .	Deep-sequencing analysis of the association between the quasispecies nature of the hepatitis C virus core region and disease progression.	<i>J Virol.</i>	87(23)	12541-51.	2013
Asahina Y, Tsuchiya K, Nishimura T, Muraoka M, Suzuki Y, Tamaki N, Yasui Y, Hosokawa T, Ueda K, Nakanishi H, Itakura J, Takahashi Y, Kurosaki M, <u>Enomoto N</u> , Nakagawa M, Kakinuma S, Watanabe M, Izumi N.	Genetic variation near interleukin 28B and the risk of hepatocellular carcinoma in patients with chronic hepatitis C.	<i>J Gastroenterol.</i>	Jul 17.	ePub	2013
Morisaka H, Motosugi U, Ichikawa T, Sano K, Ichikawa S, Araki T, <u>Enomoto N</u> .	MR-based measurements of portal vein flow and liver stiffness for predicting gastroesophageal varices.	<i>Magn Reson Med Sci.</i>	12(2)	77-86.	2013

Ichikawa S, Ichikawa T, Motosugi U, Sano K, Morisaka H, <u>Enomoto N</u> , Matsuda M, Fujii H, Araki T.	Presence of a hypovascular hepatic nodule showing hypointensity on hepatocyte-phase image is a risk factor for hypervascular hepatocellular carcinoma.	<i>J Magn Reson Imaging.</i>	39(2)	293-7.	2013
Nakanishi H, Kurosaki M, Nakanishi K, Tsuchiya K, Noda T, Tamaki N, Yasui Y, Hosokawa T, Ueda K, Itakura J, Anami K, Asahina Y, <u>Enomoto N</u> , Higuchi T, Izumi N.	Impaired brain activity in cirrhotic patients with minimal hepatic encephalopathy: Evaluation by near-infrared spectroscopy.	<i>Hepatol Res.</i>	Apr 5.	ePub	2013
Saibara T, <u>Enomoto N</u> , Kaneko S, Chayama K, Sata M, Imawari M, Onishi S, Okita K.	Clinical efficacy of combination therapy with ME3738 and pegylated interferon-alpha-2a in patients with hepatitis C virus genotype 1.	<i>Hepatol Res.</i>	Apr 19.	ePub	2013
Asahina Y, Tsuchiya K, Nishimura T, Muraoka M, Suzuki Y, Tamaki N, Yasui Y, Hosokawa T, Ueda K, Nakanishi H, Itakura J, Takahashi Y, Kurosaki M, <u>Enomoto N</u> , Nakagawa M, Kakinuma S, Watanabe M, Izumi N.	$\alpha$ -fetoprotein levels after interferon therapy and risk of hepatocarcinogenesis in chronic hepatitis C.	<i>Hepatology.</i>	58(4)	1253-62.	2013
Shindo H, Maekawa S, Komase K, Miura M, Kadokura M, Sueki R, Komatsu N, Shindo K, Amemiya F, Nakayama Y, Inoue T, Sakamoto M, Yamashita A, Moriishi K, <u>Enomoto N</u> .	IL-28B (IFN- $\lambda$ 3) and IFN- $\alpha$ synergistically inhibit HCV replication.	<i>J Viral Hepat.</i>	20(4)	281-9.	2013
Kurosaki M, Tanaka Y, Nishida N, Sakamoto N, <u>Enomoto N</u> , Matsuura K, Asahina Y, Nakagawa M, Watanabe M, Sakamoto M, Maekawa S, Tokunaga K, Mizokami M, Izumi N.	Model incorporating the ITPA genotype identifies patients at high risk of anemia and treatment failure with pegylated-interferon plus ribavirin therapy for chronic hepatitis C.	<i>J Med Virol.</i>	85(3)	449-58.	2013
Komase K, Maekawa S, Miura M, Sueki R, Kadokura M, Shindo H, Shindo K, Amemiya F, Nakayama Y, Inoue T, Sakamoto M, Yamashita A, Moriishi K, <u>Enomoto N</u> .	Serum RANTES level influences the response to pegylated interferon and ribavirin therapy in chronic hepatitis C.	<i>Hepatol Res.</i>	43(8)	865-75.	2013

<u>Kazuhiro Haraguchi</u>	Synthesis of Novel 4'-C-Methyl-1',3'-dioxolane pyrimidine nucleosides and evaluation of its anti-HIV-1 activity"	<i>Tetrahedron</i>	69	10884-10892	2013
<u>Kazuhiro Haraguchi</u>	KAY-2-41, a novel nucleoside analogue inhibitor of orthopoxviruses in vitro and in vivo	<i>Antimicrob. Agents Chemother.</i>	58	27-37	2014
Kazuki Izumi, Kumi Kawaji, Fusasko Miyamoto, Kazuki Shimane, Kazuya Shimura, Yasuko Sakagami, Toshio Hattori, Kentaro Watanabe, Shinya Oishi, Nobutaka Fujii, Masao Matsuoka, Mitsuo Kaku, Stefan G. Sarafianos, and <u>Eiichi N. Kodama</u>	Mechanism of Resistance to S138A Substituted Enfuvirtide and its Application to Peptide Design.	<i>International Journal of Biochemistry and Cell Biology</i>	45	908-915	2013
Kazuki Shimane, KumiKawaji, Fusako Miyamoto, Shinya Oishi, Kentaro Watanabe, YasukoSakagami, Nobutaka Fujii, Kazuya Shimura, Masao Matsuoka, Mitsuo Kaku, Stefan Sarafianos, and <u>Eiichi Kodama</u>	HIV-1 resistance mechanism to an electrostatically constrained peptide fusion inhibitor that is active against T-20-resistant strains.	<i>Antimicrobial Agents and Chemotherapy</i>	57	4035-4038	2013
Eleftherios Michailidis, Emily M Ryan, Atsuko Hachiya, Karen A Kirby, Bruno Marchand, Maxwell D Leslie, Andrew D Huber, Yee T Ong, Jacob C Jackson, Kamalendra Singh, <u>Eiichi N Kodama</u> , Hiroaki Mitsuya, Michael A Parniak and Stefan G Sarafianos	Hypersusceptibility Mechanism of Tenofovir-Resistant HIV to EFdA.	<i>Retrovirology</i>	10	65 doi:10.1186/1742-4690-10-65	2013
Atsuko Hachiya, Aaron Reeve, Bruno Marchand, Eleftherios Michailidis, Yee Ong, Karen Kirby, Maxwell Leslie, Shinichi Oka, <u>Eiichi Kodama</u> , Lisa Rohan, Hiroaki Mitsuya, Michael Parniak, and Stefan Sarafianos	Evaluation of combinations of 4'-ethynyl-2-fluoro-2'-deoxyadenosine with clinically used antiretroviral drugs.	<i>Antimicrobial Agents and Chemotherapy</i>	57	4554-4558	2013

Kirby KA, Michailidis E, Fetterly TL, Steinbach MA, Singh K, Marchand B, Leslie MD, Hagedorn AN, <u>Kodama EN</u> , Marquez VE, Hughes SH, Mitsuya H, Parniak MA, Sarafianos SG	Effects of substitutions at the 4' and 2 positions on the bioactivity of 4'-ethynyl-2'-deoxyadenosine.	<i>Antimicrobial Agents and Chemotherapy</i>	57	6254-64	2013
Nishida N, Sawai H, Kashiwase K, Minami M, Sugiyama M, Seto WK, Yuen MF, Posuwan N, Poovorawan Y, Ahn SH, Han KH, Matsuura K, <u>Tanaka Y</u> , Kurosaki M, Asahina Y, Izumi N, Kang JH, Hige S, Ide T, Yamamoto K, Sakaida I, Murawaki Y, Itoh Y, Tamori A, Orito E, Hiasa Y, Honda M, Kaneko S, Mita E, Suzuki K, Hino K, Tanaka E, Mochida S, Watanabe M, Eguchi Y, Masaki N, Murata K, Korenaga M, Mawatari Y, Ohashi J, Kawashima M, Tokunaga K, Mizokami M.	New Susceptibility and Resistance HLA-DP Alleles to HBV-Related Diseases Identified by a Trans-Ethnic Association Study in Asia.	<i>PLoS One.</i>	9(2)	e86449.	2014
Wong DK, Kopaniszen M, <u>Omagari K</u> , <u>Tanaka Y</u> , Fong DY, Seto WK, Fung J, Huang FY, Zhang AY, Hung IF, Lai CL, Yuen MF.	Effect of hepatitis B virus reverse transcriptase variations on entecavir treatment response. <i>J Infect Dis.</i> in press.	<i>J Infect Dis.</i>	in press		
Kitagawa W, Ozaki T, Nishioka T, <u>Yasutake Y</u> , Hata M, Nishiyama M, Kuzuyama T, Tamura T	Cloning and heterologous expression of the aurachin RE biosynthesis gene cluster afford a new cytochrome P450 for quinoline N-hydroxylation	<i>ChemBioChem</i>	14	1085-1093	2013
<u>Yasutake Y</u> , Nishioka T, Imoto N, Tamura T	A single mutation at the ferredoxin binding site of P450 Vdh enables efficient biocatalytic production of 25-hydroxyvitamin D3	<i>ChemBioChem</i>	14	2284-2291	2013
Matsumoto Y, <u>Yasutake Y</u> , Takeda Y, Tamura T, Yokota A, Wada M	Crystallization and preliminary X-ray diffraction studies of D-threo-3-hydroxyaspartate dehydratase isolated from <i>Delftia</i> sp. HT23	<i>Acta Crystallogr. Section F</i>	69	1131-1134	2013
<u>Yasutake Y</u> , Kitagawa W, Hata M, Nishioka T, Ozaki T, Nishiyama M, Kuzuyama T, Tamura T	Structure of the quinoline N-hydroxylating cytochrome P450 RauA, an essential enzyme that confers antibiotic activity on aurachin alkaloids	<i>FEBS Lett.</i>	588	105-110	2014

#### IV. 研究成果の刊行物・別刷



## Effect of albumin on transthyretin and amyloidogenic transthyretin Val30Met disposition and tissue deposition in familial amyloidotic polyneuropathy<sup>☆</sup>

Kazuaki Taguchi<sup>a,e</sup>, Hirofumi Jono<sup>g</sup>, Tomoe Kugimiya-Taguchi<sup>a</sup>, Saori Nagao<sup>a</sup>, Yu Su<sup>c</sup>, Keishi Yamasaki<sup>e,f</sup>, Mineyuki Mizuguchi<sup>h</sup>, Toru Maruyama<sup>a,b</sup>, Yukio Ando<sup>d</sup>, Masaki Otagiri<sup>a,e,f,\*</sup>

<sup>a</sup> Department of Biopharmaceutics, Graduate School of Pharmaceutical Sciences, Kumamoto University, Kumamoto, Japan

<sup>b</sup> Center for Clinical Pharmaceutical Sciences, Kumamoto University, Kumamoto, Japan

<sup>c</sup> Department of Diagnostic Medicine, Kumamoto University, Kumamoto, Japan

<sup>d</sup> Department of Neurology, Graduate School of Medical Sciences, Kumamoto University, Kumamoto, Japan

<sup>e</sup> Faculty of Pharmaceutical Sciences, Sojo University, Kumamoto, Japan

<sup>f</sup> DDS Research Institute, Sojo University, Kumamoto, Japan

<sup>g</sup> Department of Pharmacy, Kumamoto University Hospital, Kumamoto, Japan

<sup>h</sup> Faculty of Pharmaceutical Sciences, University of Toyama, Toyama, Japan

### ARTICLE INFO

#### Article history:

Received 7 August 2013

Accepted 28 October 2013

#### Keywords:

Transthyretin

Familial amyloidotic polyneuropathy

Albumin

### ABSTRACT

**Aims:** Transthyretin (TTR)-related familial amyloidotic polyneuropathy (FAP) is characterized by the systemic accumulation of amyloid fibrils caused by amyloidogenic. Our previous studies demonstrated that albumin played a role in the inhibition of TTR amyloid-formation. The aim of this study was to evaluate the effect of albumin on TTR disposition and tissue deposition *in vivo*.

**Main methods:** For pharmacokinetic studies, recombinant wild-type TTR (rTTR) and recombinant amyloidogenic TTR Val30Met (rATTR V30M) were labeled with iodine and administered to Sprague–Dawley rats and albuminemia rats (NAR: Nagase Albuminemia Rats). The deposition of ATTR V30M was also analyzed by immunohistochemistry in the transgenic (Tg) rats possessing a human *ATTR V30M gene* (ATTR V30M Tg rats) and NAR possessing a human *ATTR V30M gene* (ATTR V30M Tg NAR).

**Key findings:** The presence of albumin had no effect on the tissue distribution of either rTTR or rATTR V30M. However, more ATTR V30M was deposited in the hearts, stomachs and small intestines of ATTR V30M Tg NAR rats, compared to ATTR V30M Tg rats.

**Significance:** Although the disposition of TTR and ATTR V30M was unaffected by the presence of albumin, the deposition of ATTR V30M in some organs was apparently increased in the absence of albumin compared to the presence of albumin. These results show that albumin would contribute to suppressing the tissue deposition of TTR in pathogenesis of FAP, but does not affect the disposition of TTR.

© 2013 Elsevier Inc. All rights reserved.

### Introduction

Albumin is the most abundant protein in the blood, and an important carrier of endogenous and exogenous ligands in the circulation. It contributes to the maintenance of osmotic pressure and plasma pH and to the Donnan-effect in capillaries (Otagiri et al., 2013; Otagiri and

Chuang, 2009). In addition, the cysteine residue at position 34 (Cys34) in albumin provides antioxidant activity (Stewart et al., 2005), which, in turn, influences the plasma thiol-dependent antioxidant status of albumin, as well as the extent of oxidative damage to proteins (Quinlan et al., 1998, 2004). These multiple functions of albumin have a key role in the maintenance of physiological homeostasis. In fact, it was reported that hypoalbuminemia is strongly associated with the progression of and mortality in a number of disorders (Okamura et al., 2013; Staples et al., 2010; Zisman et al., 2009). We also reported that serum albumin levels and the reduced form at Cys34 of albumin were decreased in familial amyloidotic polyneuropathy (FAP) patients as the disease progressed (Kugimiya et al., 2011).

Transthyretin (TTR)-related FAP is an autosomal dominant form of a fatal form of heredity amyloidosis characterized by the systemic accumulation of amyloid fibrils in organs (Ando et al., 1993, 2005). To date, more than 100 different points of mutation in the TTR gene have

**Abbreviations:** TTR, transthyretin; FAP, familial amyloidotic polyneuropathy; ATTR, amyloidogenic transthyretin; NAR, Nagase Albuminemia Rats; Tg, transgenic; <sup>125</sup>I, iodine; % of ID, % of injection of dose;  $t_{1/2 \alpha}$ , distribution-phase half-life;  $t_{1/2 \beta}$ , elimination-phase half-life; CL, clearance; AUC, area under the concentration-time curve;  $V_1$ , distribution volume of central compartment;  $V_2$ , distribution volume of peripheral compartment;  $V_{dss}$ , distribution volume.

<sup>☆</sup> Albumin plays key roles in transthyretin disposition.

\* Corresponding author at: Faculty of Pharmaceutical Sciences, Sojo University, 4-22-1 Ikeda, Kumamoto 862-0082, Japan. Tel.: +81 96 326 3887; fax: +81 96 326 5048.

E-mail address: [otagirim@ph.sojo-u.ac.jp](mailto:otagirim@ph.sojo-u.ac.jp) (M. Otagiri).



been reported, and most of these mutations are amyloidogenic (Ando et al., 2005; Benson and Kincaid, 2007; Connors et al., 2003). Of the different types of amyloidogenic transthyretin (ATTR), ATTR Val30Met (ATTR V30M) is the most common (Benson and Uemichi, 1996). Although many attempts have been made to identify various types of ATTR-related FAP (Connors et al., 2003), the mechanisms responsible for the self-assembly of naturally occurring proteins into amyloid deposits remain a mystery even given the progress made in biochemical and diagnosis methods. Our previous *in vitro* studies showed that S-nitrosylated TTRs and ATTR V30M induced more amyloid fibrils than did unmodified TTRs and wild-type TTR, respectively, which indicates that oxidative stress is a facilitator of amyloid formation (Saito et al., 2005). Furthermore, we also revealed that albumin, which maintains antioxidant activity, may possibly play an inhibitory role in the TTR amyloid-formation process in organs (Kugimiya et al., 2011). However, the precise roles of albumin in the deposition of TTR in organs remain unknown.

The objective of this study was to evaluate the role of albumin in TTR disposition and tissue deposition *in vivo*. In initial experiments, we labeled recombinant TTR (rTTR) or recombinant ATTR V30M (rATTR V30M) with iodine ( $^{125}\text{I}$ ) to produce  $^{125}\text{I}$ -labeled TTR ( $^{125}\text{I}$ -rTTR) or ATTR V30M ( $^{125}\text{I}$ -rATTR V30M) and subsequently examined changes in the pharmacokinetic properties of rTTR or rATTR V30M using Sprague–Dawley (SD) rats and analbuminemia rats (NAR: Nagase Analbuminemia Rats). Next, to evaluate in detail the effect of albumin on TTR deposition, we compared the extent of TTR deposition between the transgenic (Tg) rats possessing the human ATTR V30M gene (ATTR V30M Tg rats) and NAR possessing the human ATTR V30M gene (ATTR V30M Tg NAR).

## Materials and methods

### Expression and purification of the rTTR and rATTR V30M

The rTTR and rATTR V30M were expressed and purified as reported in a previous study (Matsubara et al., 2003). In this preparation, the TTR or ATTR V30M vector (pQE30) was mixed with the *E. coli* strain M15. A preculture was grown overnight at 37 °C in Luria broth medium with ampicillin and kanamycin and was inoculated to 100 mL of the fresh Luria broth medium. Protein expression was induced with 1 mM isopropyl- $\beta$ -D-thiogalactopyranoside when the absorbance at 600 nm reached 0.6. After growth for 7 h at 37 °C with shaking, the cells were immediately chilled on ice and harvested by centrifugation at 5000 g for 20 min at 4 °C. The pelleted cells were resuspended and lysed by sonication at 4 °C. After centrifugation at 5000 g for 40 min at 4 °C, the supernatant was filtered and the proteins were isolated by passage through DEAE sepharose gel. Finally, the proteins were purified and concentrated by high performance liquid chromatography.

### rTTR and rATTR V30M labeling with $^{125}\text{I}$

The rTTR and rATTR V30M were labeled with  $^{125}\text{I}$  as previously reported, with minor modifications (Matsushita et al., 2006).  $^{125}\text{I}$ -rTTR and  $^{125}\text{I}$ -rATTR V30M were prepared by incubation of rTTR and rATTR V30M with Na $^{125}\text{I}$  (PerkinElmer Inc., Piscataway, NJ, USA) in an Iodo-Gen (1, 3, 4, 6-tetrachloro-3a, 6a-diphenylglycoluril) tube for 30 min at room temperature. Thereafter,  $^{125}\text{I}$ -rTTR and  $^{125}\text{I}$ -rATTR V30M were isolated from free  $^{125}\text{I}$  by passage through a PD-10 column (GE Healthcare Bio-Sciences AB; Patent Department Björkgatan 30, 75184 Uppsala, SE).

### The pharmacokinetic experiments

All animal experiments were performed according to the guidelines, principles, and procedures for the care and use of laboratory animals of Kumamoto University. All rats were given water

containing 5 mM sodium iodide for the duration of the experiment to avoid specific accumulation in the glandula thyreoidea. Male SD rats (Kyudou Co., Kumamoto, Japan) or NAR (Kyudou Co., Kumamoto, Japan) were anesthetized with ether and injected with the  $^{125}\text{I}$ -rTTR or  $^{125}\text{I}$ -rATTR V30M via the tail vein at a dose of 0.1 mg/kg. Blood samples were collected at multiple time points after the  $^{125}\text{I}$ -rTTR or  $^{125}\text{I}$ -rATTR V30M (10 min, 15 min, 30 min, 1.5 h, 3 h and 4 h) and the plasma was separated by centrifugation (3000 g, 5 min). Degraded rTTR or rATTR V30M and free  $^{125}\text{I}$  were removed from the plasma by centrifugation in 1% bovine serum albumin and 40% trichloroacetic acid. After obtaining the last blood sampling, the organs were excised (kidneys, liver, spleen, lungs, heart, stomach, and small intestine), rinsed with saline, and weighed. The radioactivity of the samples was determined by means of a  $\gamma$ -counter (ARC-5000, Aloka, Tokyo, Japan).

### Preparation of ATTR V30M Tg rats and ATTR V30M Tg NAR

NAR were isolated from SD rats of CLEA Japan (Japan CLEA Co., Kanagawa, Japan) (Nagase et al., 1979). ATTR V30M Tg rats were generated as previously described (Ueda et al., 2007). The ATTR V30M Tg NAR were developed by mating NAR and V30M Tg rats and were genotyped by a PCR analysis of ear DNA. The animals were maintained in a specific pathogen-free environment at the Center for Animal Resources and Development, Kumamoto University.

### Immunohistochemical staining

9-month-old ATTR V30M Tg rats and ATTR V30M Tg NAR were sacrificed by acute bleeding from the abdominal aorta and selected organs (kidneys, liver, spleen, lungs, heart, stomach and small intestine) removed. The organs were then resected *en bloc* for immunohistochemical staining. The organs were fixed in 4% paraformaldehyde overnight and embedded in paraffin.

Paraffin-embedded 4  $\mu\text{m}$ -thick sections were prepared and deparaffinated in xylene and rehydrated in a graded series of alcohols. Deparaffinized sections were pretreated by heating for 20 min in an autoclave apparatus. The slides were then treated with periodic acid for 10 min at room temperature, after which they were incubated in 5% normal serum for 1 h at room temperature in a moist chamber. The primary antibodies were rabbit polyclonal anti-TTR (Dako, Glostrup, Denmark) and were used at a 1:50 dilution. The secondary antibody was a horseradish peroxidase-conjugated goat anti-rabbit immunoglobulin antibody (Dako, Glostrup, Denmark) diluted 1:100 in buffer. Reactivity was visualized with the DAB Liquid System (Dako, Glostrup, Denmark). Sections were counterstained with hematoxylin.

### Histopathological scoring system of TTR deposition in organs

The sections were examined by light microscopy. For each organ, 5 different selected areas per specimen used for semiquantitative immunohistochemistry were analyzed by two independent investigators blind manner. The deposition of TTR in organs was assessed according to the degree of deposition using a 0 to 2 grading system. A score of 0 indicates the absence of deposition, a score of 1 indicates mild deposition (<50% of the total muscle layer in visual field), a score of 2 corresponds to severe deposition (>50% of the total muscle layer in visual field). Scores for each organ were then averaged per group (ATTR V30M Tg rats and ATTR V30M Tg NAR).

### Data analysis

A two-compartment model was used for the pharmacokinetic analysis after the administration of  $^{125}\text{I}$ -rTTR or  $^{125}\text{I}$ -rATTR V30M. Each parameter was calculated by fitting using MULTI, a normal least-squares program (Yamaoka et al., 1981). Data are reported as the mean  $\pm$  SD

for the indicated number of animals. Significant differences among each group were examined using the Student's *t*-test. A probability value of  $p < 0.05$  was considered to indicate statistical significance.

## Results

### Pharmacokinetic study of rTTR with or without albumin

Fig. 1A shows the time course for the plasma concentration of  $^{125}\text{I}$ -rTTR that had been injected into SD rats or NAR at a dose of 0.1 mg/kg, and Table 1 lists the pharmacokinetic parameters obtained using the two-compartment model. The plasma concentration curves and pharmacokinetic parameters of  $^{125}\text{I}$ -rTTR were similar between the SD rats and NAR (elimination-phase half-life ( $t_{1/2\beta}$ );  $2.53 \pm 0.26$  and  $3.02 \pm 0.39$  h, for the SD rats and NAR, respectively).

Fig. 1B shows the tissue distribution of the  $^{125}\text{I}$ -rTTR (% of injection of dose (% of ID)) at 4 h after administration to SD rats or NAR.  $^{125}\text{I}$ -rTTR was distributed at relatively high levels in kidneys, liver, stomach and small intestine in both SD rats and NAR. However, no significant difference in the amount of  $^{125}\text{I}$ -rTTR between the SD rats and NAR was observed in any of the organs.

### Pharmacokinetic study of rATTR V30M with or without albumin

A pharmacokinetic study of rATTR V30M was also performed in SD rats and NAR. As shown in Fig. 2A, the plasma concentration of  $^{125}\text{I}$ -rATTR V30M in NAR was essentially the same as that in SD rats. With the change in plasma concentration of  $^{125}\text{I}$ -rATTR V30M, the pharmacokinetic parameters for NAR were also similar to that in SD rats (Table 2). However, the pharmacokinetic parameters were obviously different between administration of  $^{125}\text{I}$ -rTTR and  $^{125}\text{I}$ -rATTR V30M in both SD rats

**Table 1**

Pharmacokinetic parameters after the administration of  $^{125}\text{I}$ -TTR by an intravenous injection to SD rats or NARs. Both SD rats and NARs received a single injection of  $^{125}\text{I}$ -TTR at a dose of 0.1 mg/kg. At each time after the injection of  $^{125}\text{I}$ -TTR, a blood sample was collected from the tail vein, and plasma was obtained. Each parameter was calculated by MULTI using a two-compartment model.

	SD rat	NAR
$t_{1/2\alpha}$ (h)	$0.12 \pm 0.02$	$0.13 \pm 0.03$
$t_{1/2\beta}$ (h)	$2.53 \pm 0.26$	$3.02 \pm 0.39^{\#}$
CL (mL/h)	$9.33 \pm 0.99$	$8.69 \pm 0.79$
AUC (h *% of dose/mL)	$10.8 \pm 1.15$	$11.6 \pm 1.07$
$V_1$ (mL)	$8.45 \pm 0.66$	$8.26 \pm 2.14$
$V_2$ (mL)	$20.7 \pm 3.6$	$23.7 \pm 3.5$
$V_{\text{dss}}$ (mL)	$29.2 \pm 3.7$	$31.9 \pm 4.4$

Each value represents the mean  $\pm$  S.D. ( $n = 6$ ).

$t_{1/2\alpha}$ : the distribution-phase half-life,  $t_{1/2\beta}$ : the elimination-phase half-life, CL: clearance, AUC: area under the concentration-time curve,  $V_1$ : distribution volume of central compartment,  $V_2$ : distribution volume of peripheral compartment,  $V_{\text{dss}}$ : distribution volume.  
<sup>#</sup>  $p < 0.05$  vs SD rat.

and NAR: the area under the concentration-time curve (AUC) for  $^{125}\text{I}$ -rATTR V30M was decreased compared to that for  $^{125}\text{I}$ -rTTR, and the distribution volume ( $V_{\text{dss}}$ ), the distribution volume of the central compartment ( $V_1$ ) and the peripheral compartment ( $V_2$ ), the clearance (CL) of  $^{125}\text{I}$ -rATTR V30M were increased compared to that of  $^{125}\text{I}$ -rTTR (Tables 1 and 2).

As shown in Fig. 2B, the  $^{125}\text{I}$ -rATTR V30M in both SD rats and NAR was mainly distributed in the kidneys, liver, stomach and small intestine, similar to the case of  $^{125}\text{I}$ -rTTR. Among the organs observed, no significant differences in the distribution of  $^{125}\text{I}$ -rATTR V30M between the SD rats and NAR were found.

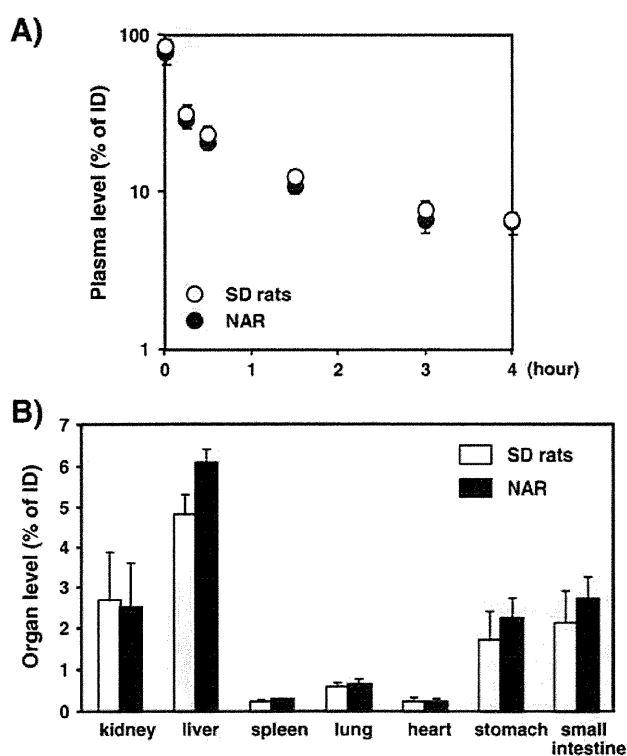


**Fig. 1.** (A) The time course for the relative plasma concentration of  $^{125}\text{I}$ -rTTR after i.v. administration to SD rats (open circle) and NAR (closed circle). (B) Tissue distribution of radioactivity at 4 hours after i.v. administration of  $^{125}\text{I}$ -rTTR to SD rats (open bar) and NAR (closed bar).  $^{125}\text{I}$ -rTTR were injected to SD rats ( $n = 6$ ) and NAR ( $n = 6$ ) at a dose of 0.1 mg/kg. The radioactivities were determined using a  $\gamma$ -counter. Each data point represents the mean  $\pm$  S.D. % of ID: % of injection of dose.

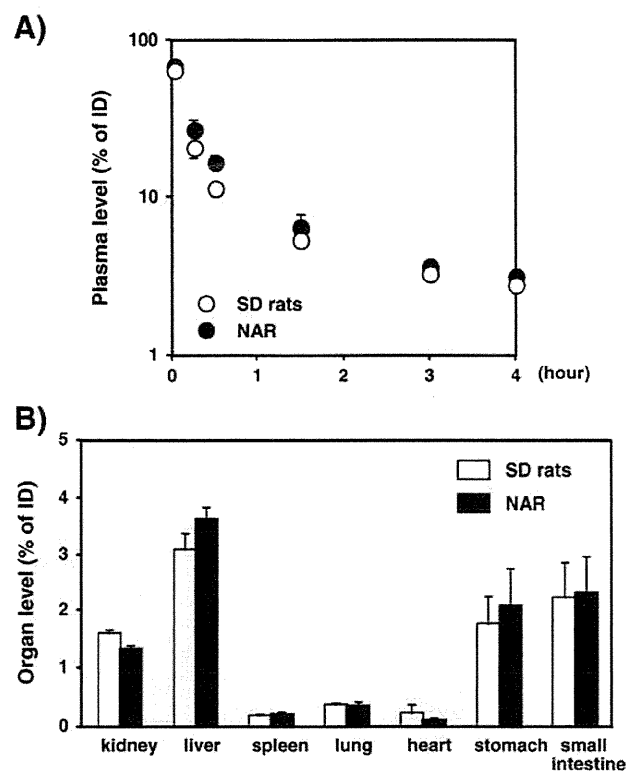


**Fig. 2.** (A) The time course for the relative plasma concentration of  $^{125}\text{I}$ -rATTR V30M after i.v. administration to SD rats (open circle) and NAR (closed circle). (B) Tissue distribution of radioactivity at 4 h after i.v. administration of  $^{125}\text{I}$ -rATTR V30M to SD rats (open bar) and NAR (closed bar).  $^{125}\text{I}$ -rATTR V30M were injected to SD rats ( $n = 3$ ) and NAR ( $n = 4$ ) at a dose of 0.1 mg/kg. The radioactivities were determined using a  $\gamma$ -counter. Each data point represents the mean  $\pm$  S.D. % of ID: % of injection of dose.

**Table 2**

Pharmacokinetic parameters after the administration of  $^{125}\text{I}$ -ATTR V30M by an intravenous injection to SD rats or NARs. Both SD rats and NARs received a single injection of  $^{125}\text{I}$ -ATTR V30M at a dose of 0.1 mg/kg. At each time after the injection of  $^{125}\text{I}$ -ATTR V30M, a blood sample was collected from the tail vein, and plasma was obtained. Each parameter was calculated by MULTI using a two-compartment model.

	SD	NAR
$t_{1/2\alpha}$ (h)	0.12 ± 0.01	0.17 ± 0.04
$t_{1/2\beta}$ (h)	2.61 ± 0.25	3.16 ± 1.06
CL (mL/h)	23.4 ± 1.9	17.6 ± 2.0*
AUC (h *% of dose/mL)	4.29 ± 0.36	5.74 ± 0.59*
$V_1$ (mL)	13.9 ± 1.7	12.6 ± 1.1
$V_2$ (mL)	52.5 ± 9.3	44.1 ± 13.6
$V_{ss}$ (mL)	66.4 ± 11.0	56.7 ± 14.5

Each value represents the mean ± S.D. (SD rats;  $n = 3$ , NAR;  $n = 4$ ).

$t_{1/2\alpha}$ : the distribution-phase half-life,  $t_{1/2\beta}$ : the elimination-phase half-life, CL: clearance, AUC: area under the concentration-time curve,  $V_1$ : distribution volume of central compartment,  $V_2$ : distribution volume of peripheral compartment,  $V_{ss}$ : distribution volume.

\*  $p < 0.05$  vs SD rat.

#### ATTR V30M deposition in ATTR V30M Tg rats and ATTR V30M Tg NAR

We further evaluated the effect of albumin on the deposition of ATTR V30M in the organs (kidneys, liver, spleen, heart, lungs, stomach and small intestine) using ATTR V30M Tg rats and ATTR V30M Tg NAR. As

a result, the score of degree of ATTR V30M deposition in the heart, stomach and small intestine of the ATTR V30M Tg NAR was significantly higher than that of the ATTR V30M Tg rats (Fig. 3), while deposition of ATTR V30M in other organs (kidneys, liver, spleen and lungs) was not observed in both groups (data not shown). Furthermore, the deposits in the heart, stomach and small intestine were almost entirely localized to the muscle layer, including the myocardial layer, gastric muscularis and the muscular coat of the small intestine, respectively (Fig. 3). These data strongly suggest the possibility that the presence of albumin contributes to the inhibition of ATTR V30M deposition in tissues.

#### Discussion

The major finding of this study is that the presence of albumin inhibits the ATTR V30M deposition process in organs rather than effect on the pharmacokinetic properties (plasma concentration and tissue distribution) of rTTR and rATTR V30M.

TTR weighs 55 kDa and is a tetramer composed of four identical monomer subunits. Each monomer is 127 amino acid residues long (Peterson et al., 1998). It is mainly biosynthesized in the liver, and, in normal healthy individuals, the basal level of TTR is maintained at approximately 20–40 mg/dL. Although TTR normally binds to the retinol binding protein and thyroxine in plasma, which suppresses their excretion from the kidney and behave as a transporter (Boomsma et al., 1991;

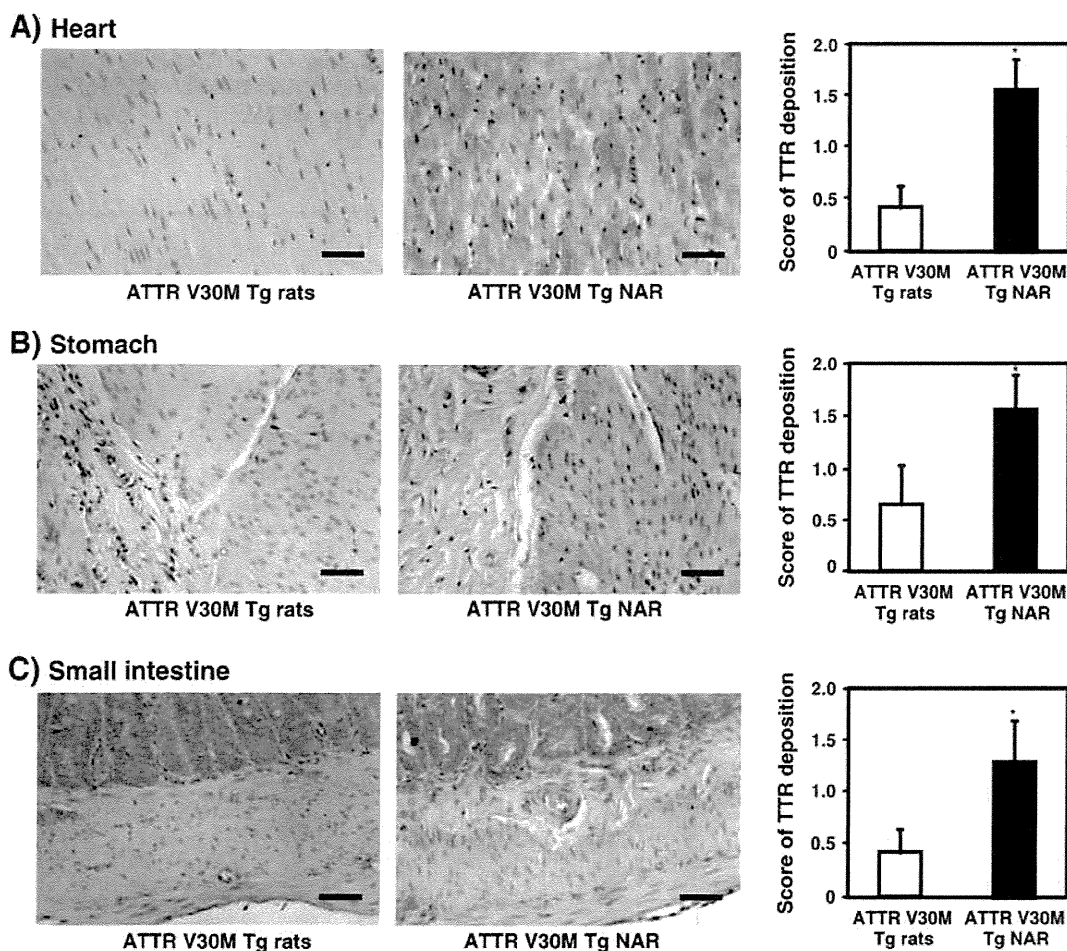


**Fig. 3.** Immunohistochemistry for human ATTR V30M and the score for the degree of TTR deposition in heart (A), stomach (B) and small intestine (C) of the transgenic (Tg) rats possessing a human *ATTR V30M* gene (ATTR V30M Tg rats) and analbuminemia rats possessing a human *ATTR V30M* gene (ATTR V30M Tg NAR). Immunoreactivity with rabbit polyclonal anti-human TTR antibody in the heart, stomach and small intestine of ATTR V30M Tg rats and V30M Tg NAR at 9 months after birth. The left panels shown are representative images of heart (A), stomach (B) and small intestine (C) collected from ATTR V30M Tg rats and ATTR V30M Tg NAR. Scale bars = 50  $\mu\text{m}$ . The right panels shown are semiquantitative analysis of TTR deposition in each organ of ATTR V30M Tg rats and ATTR V30M Tg NAR. The volume of TTR deposition is classified into the following 3 grades: 0 corresponded with absence of deposition, a score of 1 indicated the mild deposition, a score of 2 corresponds to severe deposition. Each bar represents the mean ± SD ( $n = 5$ ). \* $p < 0.01$  vs ATTR V30M Tg rats.

Monaco et al., 1995; Pettersson et al., 1995), its amyloidogenesis, especially ATTR V30M is the major amyloidogenic source for FAP, representing the major causative agent of FAP. It is also well-known that albumin is the most abundant protein in plasma, and has multiple functions. Among the functional properties of albumin, the binding of numerous endogenous and exogenous compounds is one of its important roles, and this property ultimately exerts a significant degree of influence on their disposition (Otagiri et al., 2013; Otagiri and Chuang, 2009). In our previous study involving the binding of TTR to various plasma proteins using BIAcore analysis, albumin had a higher binding affinity for TTR (dissociation-rate constants ( $K_d$ ) =  $1.49 \times 10^{-3}$  M) than other proteins (such as,  $\alpha$ -1 acid glycoprotein and transferrin) (Kugimiya et al., 2011), which indicates the possibility that it is associated with the regulation of TTR disposition, for example the tissue distribution of TTR after being released into the blood circulation from the liver, where albumin would function as a transporter. Contrary to our hypothesis, the present pharmacokinetic study demonstrated that the disposition, was not significantly affected by the plasma concentration and tissue distribution of both rATTR and ATTR V30M between rats with and without albumin (Figs. 1 and 2). These results indicate that the presence of albumin had no effect on the disposition of rATTR and ATTR V30M.

Interestingly, the AUC for  $^{125}\text{I}$ -ATTR V30M was decreased compared to that of  $^{125}\text{I}$ -rATTR in both SD rats and NAR, while each distribution volume ( $V_1$ ,  $V_2$  and  $V_{ss}$ ) and the CL of  $^{125}\text{I}$ -ATTR V30M was increased compared to that of  $^{125}\text{I}$ -rATTR in both SD rats and NAR (Tables 1 and 2). In a previous study, Longo Alves et al. (1997) reported that ATTR V30M had a faster CL than TTR T119M, which is known as a non-amyloidogenic TTR variant, and ATTR V30M had a lower stability than TTR T119M. Based on these findings, they concluded that these physical differences between ATTR V30M and TTR T119M may be an important factor in amyloidogenesis. It was reported that ATTR V30M is the most common amyloidogenic mutation (Benson and Uemichi, 1996), while wild-type TTR is a non-amyloidogenic TTR. In addition, the stability of ATTR V30M was lower than that of non-mutated TTR (Zhang et al., 2013). Taken together these findings indicate that the pharmacokinetic difference between ATTR V30M and wild-type TTR possibly involves a higher systemic accumulation of amyloid fibrils derived from ATTR V30M than non-mutated TTR. Further investigations will be needed to elucidate the detailed mechanism responsible for the kinetic differences between rATTR V30M and rATTR, and whether these kinetic changes between variants relate to the progression of FAP.

In a previous study, we reported that ATTR V30M Tg NAR showed a tendency to exhibit more severe ATTR V30M deposition in the colon than the ATTR V30M Tg rats (Kugimiya et al., 2011). In patients with systemic amyloidosis, including FAP, amyloid deposition in not only the colon but also the heart and throughout the entire gastrointestinal tract wall is a common finding (Ikeda et al., 2002). Thus, to better understand the effect of albumin on the deposition of ATTR V30M in some organs, we examined the issue of whether ATTR V30M Tg NAR showed a higher deposition of ATTR V30M in organs (kidneys, liver, spleen, heart, lungs, stomach and small intestine) than that in ATTR V30M Tg rats. The findings indicate that in ATTR V30M Tg NAR, there was apparently more ATTR V30M deposition in the muscle layer of the heart, stomach, small intestine than ATTR V30M Tg rats (Fig. 3). This finding indicates that the absence of albumin accelerated ATTR V30M deposition. It was reported that FAP patients show malnutrition and/or renal disorders as a result of amyloid deposition in the gastrointestinal tracts and kidney, which causes the induction of hypoalbuminemia (Benson and Wallace, 1989; Margaron and Soni, 1998; Nakazato et al., 1986). Furthermore, oxidative stress plays a crucial role in the pathogenesis of FAP (Fiszman et al., 2003). Since albumin functions as an antioxidant unless Cys34 is not maintained (Otagiri and Chuang, 2009), it is possible that the quantitative and qualitative loss of albumin, especially antioxidant activity, may be associated with the process of the FAP progression. In fact, the serum albumin levels and the total reduced form of albumin, considered

as the redox state of Cys34 in albumin, decreased in patients with FAP with the progression of the disease (Kugimiya et al., 2011). Moreover, TTR also caused amyloid fibril formation in senile systemic amyloidosis (Westermarck et al., 1990), which has been shown to affect to some degree 25% of the population greater than 80 years of age (Cornwell et al., 1983). It is well documented that serum albumin levels decrease with aging (Peters, 1996). Taken together, although details of the mechanism for amyloid formation in senile systemic amyloidosis have also not been clarified (Cornwell et al., 1988), the maintenance of serum albumin levels may possibly prevent the onset of, not only FAP, but also senile systemic amyloidosis.

In conclusion, the findings reported herein indicate that albumin plays key roles in the deposition of TTR except for the possible effects of TTR pharmacokinetics. Because TTR is predominantly biosynthesized in the liver, liver transplantation is thought to be the only promising and effective symptomatic therapy (Ando, 2005; Ando et al., 1995; Holmgren et al., 1993). In the present circumstances, liver transplantation is hampered by shortages of donor organs and disparity exists between the number of donated organs and patients waiting for liver transplants. Therefore, it would be desirable to develop simple and convenient practical alternative therapies based on the precise mechanism for amyloid fibril formation, but no practical alternatives have yet been developed. Clinically, albumin is commercially available as a plasma expander, and also the administration of albumin is generally considered to be the gold standard for treating severe hypoalbuminemia as a result of conditions such as burns, the nephritic syndrome, reduction in the synthesis of albumin induced by chronic liver cirrhosis and hemorrhagic shock. Hence, it would be expected that albumin administration at early stage of FAP could be a new type of pharmaceutical therapy that would arrest FAP in patients with this syndrome.

#### Conflict of interest statement

No conflicts of interest were declared.

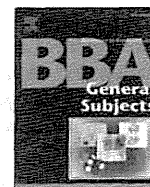
#### Acknowledgments

The authors thank Mrs. Hiroko Katsura for tissue specimen preparation. This work was supported by Grants-in-Aid for Scientific Research (B) 17390254 and (B) 21390270 from the Ministry of Education, Science, Sports and Culture of Japan.

#### References

- Ando Y. Liver transplantation and new therapeutic approaches for familial amyloidotic polyneuropathy (FAP). *Med Mol Morphol* 2005;38:142–54.
- Ando Y, Araki S, Ando M. Transthyretin and familial amyloidotic polyneuropathy. *Intern Med* 1993;32:920–2.
- Ando Y, Tanaka Y, Ando E, Yamashita T, Nishida Y, Tashima K, et al. Effect of liver transplantation on autonomic dysfunction in familial amyloidotic polyneuropathy type I. *Lancet* 1995;345:195–6.
- Ando Y, Nakamura M, Araki S. Transthyretin-related familial amyloidotic polyneuropathy. *Arch Neurol* 2005;62:1057–62.
- Benson MD, Kincaid JC. The molecular biology and clinical features of amyloid neuropathy. *Muscle Nerve* 2007;36:411–23.
- Benson MD, Uemichi T. Transthyretin amyloidosis. *Amyloid* 1996;3:44–56.
- Benson MD, Wallace MR. Genetic amyloidosis: recent advances. *Adv Nephrol Necker Hosp* 1989;18:129–37.
- Boomsma F, Man in 't Veld AJ, Schalekamp MA. Not norepinephrine but its oxidation products bind specifically to plasma proteins. *J Pharmacol Exp Ther* 1991;259:551–7.
- Connors LH, Lim A, Prokava T, Roskens VA, Costello CE. Tabulation of human transthyretin (TTR) variants, 2003. *Amyloid* 2003;10:160–84.
- Cornwell III GG, Murdoch WL, Kyle RA, Westermarck P, Pitkanen P. Frequency and distribution of senile cardiovascular amyloid. A clinicopathologic correlation. *Am J Med* 1983;75:618–23.
- Cornwell III GG, Sletten K, Johansson B, Westermarck P. Evidence that the amyloid fibril protein in senile systemic amyloidosis is derived from normal prealbumin. *Biochem Biophys Res Commun* 1988;154:648–53.
- Fiszman ML, Di Egidio M, Ricart KC, Repetto MG, Borodinsky LN, Uesuy SF, et al. Evidence of oxidative stress in familial amyloidotic polyneuropathy type 1. *Arch Neurol* 2003;60:593–7.

- Holmgren G, Ericzon BG, Groth CG, Steen L, Suhr O, Andersen O, et al. Clinical improvement and amyloid regression after liver transplantation in hereditary transthyretin amyloidosis. *Lancet* 1993;341:1113–6.
- Ikeda S, Nakazato M, Ando Y, Sobue G. Familial transthyretin-type amyloid polyneuropathy in Japan: clinical and genetic heterogeneity. *Neurology* 2002;58:1001–7.
- Kugimiya T, Jono H, Saito S, Maruyama T, Kadowaki D, Misumi Y, et al. Loss of functional albumin triggers acceleration of transthyretin amyloid fibril formation in familial amyloidotic polyneuropathy. *Lab Invest* 2011;91:1219–28.
- Longo Alves I, Hays MT, Saraiva MJ. Comparative stability and clearance of [Met30] transthyretin and [Met119]transthyretin. *Eur J Biochem* 1997;249:662–8.
- Margaron MP, Soni N. Serum albumin: touchstone or totem? *Anaesthesia* 1998;53:789–803.
- Matsubara K, Mizuguchi M, Kawano K. Expression of a synthetic gene encoding human transthyretin in *Escherichia coli*. *Protein Expr Purif* 2003;30:55–61.
- Matsushita S, Chuang VT, Kanazawa M, Tanase S, Kawai K, Maruyama T, et al. Recombinant human serum albumin dimer has high blood circulation activity and low vascular permeability in comparison with native human serum albumin. *Pharm Res* 2006;23:882–91.
- Monaco HL, Rizzi M, Coda A. Structure of a complex of two plasma proteins: transthyretin and retinol-binding protein. *Science* 1995;268:1039–41.
- Nagase S, Shimamune K, Shumiya S. Albumin-deficient rat mutant. *Science* 1979;205:590–1.
- Nakazato M, Kurihara T, Matsukura S, Kangawa K, Matsuo H. Diagnostic radioimmunoassay for familial amyloidotic polyneuropathy before clinical onset. *J Clin Invest* 1986;77:1699–703.
- Okamura K, Nagata N, Wakamatsu K, Yonemoto K, Ikegame S, Kajiki A, et al. Hypoalbuminemia and lymphocytopenia are predictive risk factors for in-hospital mortality in patients with tuberculosis. *Intern Med* 2013;52:439–44.
- Otagiri M, Chuang VT. Pharmaceutically important pre- and posttranslational modifications on human serum albumin. *Biol Pharm Bull* 2009;32:527–34.
- Otagiri M, Chuang VT, Maruyama T, Kragh-Hansen U. Human serum albumin: new insight on its structural dynamics, functional impacts and pharmaceutical applications. Kumamoto: Sojo University Publishing Center; 2013.
- Peters Jr T. All about albumin: biochemistry, genetics, and medical applications. San Diego, California: Academic Press; 1996.
- Peterson SA, Klabunde T, Lashuel HA, Purkey H, Sacchettini JC, Kelly JW. Inhibiting transthyretin conformational changes that lead to amyloid fibril formation. *Proc Natl Acad Sci U S A* 1998;95:12956–60.
- Pettersson T, Ernstrom U, Griffiths W, Sjoval J, Bergman T, Jornvall H. Lutein associated with a transthyretin indicates carotenoid derivatation and novel multiplicity of transthyretin ligands. *FEBS Lett* 1995;365:23–6.
- Quinlan GJ, Margaron MP, Mumby S, Evans TW, Gutteridge JM. Administration of albumin to patients with sepsis syndrome: a possible beneficial role in plasma thiol repletion. *Clin Sci (Lond)* 1998;95:459–65.
- Quinlan GJ, Mumby S, Martin GS, Bernard GR, Gutteridge JM, Evans TW. Albumin influences total plasma antioxidant capacity favorably in patients with acute lung injury. *Crit Care Med* 2004;32:755–9.
- Saito S, Ando Y, Nakamura M, Ueda M, Kim J, Ishima Y, et al. Effect of nitric oxide in amyloid fibril formation on transthyretin-related amyloidosis. *Biochemistry* 2005;44:11122–9.
- Staples AO, Greenbaum LA, Smith JM, Gipson DS, Filler G, Warady BA, et al. Association between clinical risk factors and progression of chronic kidney disease in children. *Clin J Am Soc Nephrol* 2010;5:2172–9.
- Stewart AJ, Blindauer CA, Berezenko S, Sleep D, Tooth D, Sadler PJ. Role of Tyr84 in controlling the reactivity of Cys34 of human albumin. *FEBS J* 2005;272:353–62.
- Ueda M, Ando Y, Hakamata Y, Nakamura M, Yamashita T, Obayashi K, et al. A transgenic rat with the human ATTR V30M: a novel tool for analyses of ATTR metabolisms. *Biochem Biophys Res Commun* 2007;352:299–304.
- Westermarck P, Sletten K, Johansson B, Cornwell III GG. Fibril in senile systemic amyloidosis is derived from normal transthyretin. *Proc Natl Acad Sci U S A* 1990;87:2843–5.
- Yamaoka K, Tanigawara Y, Nakagawa T, Uno T. A pharmacokinetic analysis program (multi) for microcomputer. *J Pharmacobiodyn* 1981;4:879–85.
- Zhang F, Hu C, Dong Y, Lin MS, Liu J, Jiang X, et al. The impact of V30A mutation on transthyretin protein structural stability and cytotoxicity against neuroblastoma cells. *Arch Biochem Biophys* 2013;535:120–7.
- Zisman DA, Kawut SM, Lederer DJ, Belperio JA, Lynch III JP, Schwarz MI, et al. Serum albumin concentration and waiting list mortality in idiopathic interstitial pneumonia. *Chest* 2009;135:929–35.



## Review

Albumin–drug interaction and its clinical implication<sup>☆</sup>Keishi Yamasaki<sup>a,b</sup>, Victor Tuan Giam Chuang<sup>c</sup>, Toru Maruyama<sup>d,e</sup>, Masaki Otagiri<sup>a,b,\*</sup><sup>a</sup> Faculty of Pharmaceutical Sciences, Sojo University, 4-22-1 Ikeda, Kumamoto 860-0082, Japan<sup>b</sup> DDS Research Institute, Sojo University, 4-22-1 Ikeda, Kumamoto 860-0082, Japan<sup>c</sup> School of Pharmacy, Curtin Health Innovation Research Institute, Faculty of Health Sciences, Curtin University, GPO Box U1987, Perth, Western Australia 6845, Australia<sup>d</sup> Department of Biopharmaceutics, Graduate School of Pharmaceutical Sciences, Kumamoto University, 5-1 Oe-honmachi, Kumamoto 862-0973, Japan<sup>e</sup> Center for Clinical Pharmaceutical Science, Kumamoto University, 5-1 Oe-honmachi, Kumamoto 862-0973, Japan

## ARTICLE INFO

## Article history:

Received 5 March 2013

Received in revised form 30 April 2013

Accepted 2 May 2013

Available online 10 May 2013

## Keywords:

Human serum albumin

Binding site

Displacement

Structure–function relationship

Extracorporeal albumin dialysis

## ABSTRACT

**Background:** Human serum albumin acts as a reservoir and transport protein for endogenous (e.g. fatty acids or bilirubin) and exogenous compounds (e.g. drugs or nutrients) in the blood. The binding of a drug to albumin is a major determinant of its pharmacokinetic and pharmacodynamic profile.

**Scope of review:** The present review discusses recent findings regarding the nature of drug binding sites, drug–albumin binding in certain diseased states or in the presence of coadministered drugs, and the potential of utilizing albumin–drug interactions in clinical applications.

**Major conclusions:** Drug–albumin interactions appear to predominantly occur at one or two specific binding sites. The nature of these drug binding sites has been fundamentally investigated as to location, size, charge, hydrophobicity or changes that can occur under conditions such as the content of the endogenous substances in question. Such findings can be useful tools for the analysis of drug–drug interactions or protein binding in diseased states. A change in protein binding is not always a problem in terms of drug therapy, but it can be used to enhance the efficacy of therapeutic agents or to enhance the accumulation of radiopharmaceuticals to targets for diagnostic purposes. Furthermore, several extracorporeal dialysis procedures using albumin-containing dialysates have proven to be an effective tool for removing endogenous toxins or overdosed drugs from patients.

**General significance:** Recent findings related to albumin–drug interactions as described in this review are useful for providing safer and efficient therapies and diagnoses in clinical settings. This article is part of a Special Issue entitled Serum Albumin.

© 2013 Elsevier B.V. All rights reserved.

## 1. Introduction

Human serum albumin (HSA) is a major protein component of blood plasma and plays an important role in the regulation of colloidal osmotic pressure and the transport of numerous endogenous compounds such as fatty acids, hormones, toxic metabolites (e.g. bilirubin), bile acids, amino acids, and metals [1–4]. HSA also binds a wide variety of drug molecules [1,3,5,6]. Drug molecules in the general circulation are either bound to plasma proteins or exist in unbound (free) form. Depending on the chemical properties of the drug molecules, unbound drugs can passively diffuse through the barriers constituted by endothelial cells and tissue cells into organ tissue and undergo metabolism, biliary excretion or glomerular filtration in kidney [7,8]. The unbound drugs can also be distributed intracellularly via specific transport systems (e.g. receptor-mediated endocytosis, protein-mediated transport).

**Abbreviations:** HSA, human serum albumin; 6-MNA, 6-methoxy naphthalene acetic acid; CYP, cytochrome P450

<sup>☆</sup> This article is part of a Special Issue entitled Serum Albumin.

\* Corresponding author at: Faculty of Pharmaceutical Sciences, Sojo University, 4-22-1 Ikeda, Kumamoto 860-0082, Japan. Tel.: +81 96 326 3887; fax: +81 96 326 5048.

E-mail address: [otagiri@ph.sojo-u.ac.jp](mailto:otagiri@ph.sojo-u.ac.jp) (M. Otagiri).

Only free drug molecules interact with therapeutic targets (e.g. receptors) to produce therapeutic effects [9]. In most cases, the tissue unbound concentration is in proportion to the plasma unbound concentration of drug. Thus, serum albumin–drug binding is an important factor in our understanding of the pharmacokinetics and pharmacological effects of drugs [5,10–12].

Drugs that bind to HSA with high affinities usually interact with one or two specific sites on the protein. The nature of these sites has been a subject of investigation [1,3,5,6,13]. Recent X-ray crystallographic data clearly demonstrated the location of these sites on HSA [6,14]. Changes in protein binding are often discussed based on this binding site concept. Competitive displacement between coadministered drugs which share the same binding site is a typical example [3,5]. Such knowledge of drug binding sites is one of the important issues for analyzing the mechanism of altered pharmacological effect accompanied with altered protein binding.

The binding of many drugs to HSA in patients can be changed by diseased states (e.g. renal and liver diseases) [2,5,15]. Understanding the pharmacokinetics and pharmacological activity of a drug in a diseased state is important and useful in terms of providing patients with effective medications. In addition, diagnoses and novel therapy

using drug–albumin interactions or drug–drug interactions at protein binding level are expected to produce a more effective treatment for patients. Thus, understanding drug–albumin interactions has become important for optimal therapy.

In this review, the nature of binding sites on HSA and mechanism of drug binding to HSA will be described. Furthermore, drug–HSA binding in certain diseased states or in the presence of coadministered drugs, and the possible utility of HSA in clinical applications will be described.

## 2. Drug binding to human serum albumin

HSA is a single-chain, non-glycosylated polypeptide that contains 585 amino acids with a molecular weight of 66,500 Da. Crystallographic data show that HSA contains three structurally similar  $\alpha$ -helical domains, i.e., I–III, which can be further divided into subdomains A and B (Fig. 1) [1,14,16]. The polypeptide chain forms a heart-shaped structure with an approximate dimension of  $80 \times 80 \times 30$  Å [17]. HSA contains 35 cysteine residues, and all of these except one, Cys34 (in domain I), are involved in disulfide bond formation that serves to stabilize HSA. Crystallographic data also show that interdomain and intersubdomain interactions contribute significantly to the stability of the HSA molecule.

Pioneering studies by Sudlow using a fluorescent probe displacement method in 1975 and 1976 showed the presence of two specific drug binding sites, namely, site I (also called the warfarin binding site) and site II (the benzodiazepine binding site) on HSA through screening [18,19]. These excellent studies accelerated the topology analysis and mapping of the drug binding sites on HSA. Bos et al. proposed that sites I and II are located in domains II and III, respectively, using albumin fragments derived from pepsin and trypsin digestions [20,21]. At present, through crystallographic studies, the locations of sites I and II are assigned to subdomains IIA and IIIA, respectively [1,14,16]. The entrance to site I in subdomain IIA faces subdomain IIIA [6,13,22]. Furthermore, the site has an extended binding region owing to the residues from subdomain IIB and IIIA. In contrast to site I with an entrance with contribution from different neighboring subdomains, the involvement of other subdomains in the drug-binding capacity of site II in subdomain IIIA is relatively modest. The entrance to site II is completely open to solvent, where salt-bridges

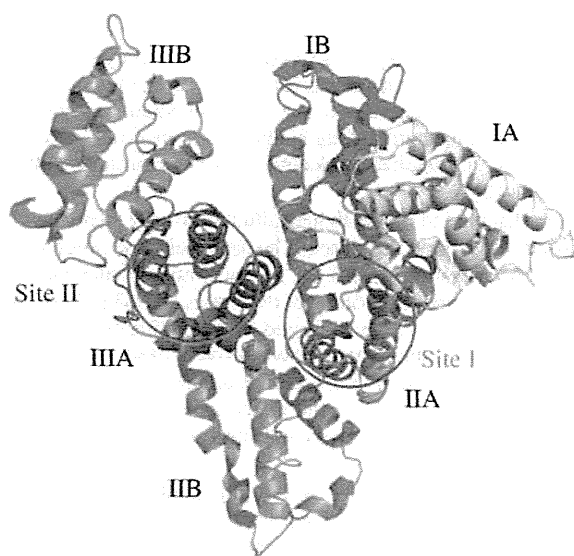
from Glu450 and Arg485 (in subdomain IIIA) to Arg348 and Glu383 (in subdomain IIB), respectively, stabilize the flanking wall of the pocket close to the entrance.

### 2.1. Site I

After the seminal work by Sudlow [18,19], a number of studies were directed toward characterizing the environment of site I. Initially, Fehske et al. reported that site I contains a warfarin–azapropazone binding area, consisting of two overlapping binding sites for warfarin and azapropazone [23–25]. They also showed the existence of a lone tryptophan residue, Trp214, in the non-overlapping part of the warfarin site. Similarly, Yamasaki et al. proposed three binding regions, subsite Ia, Ib and Ic within site I [26]. Results from other studies also indicated the presence of two independent binding regions within this site [27–30]. Ligands that strongly bound to site I are generally believed to be dicarboxylic acids and/or bulky heterocyclic molecules with a negative charge localized in the middle of the molecule (Table 1) [3,5,22]. Kragh-Hansen described this site as “a large and flexible region” based on the diversity of interaction ligands and the apparent ability to accommodate more than one of them at a time [29]. Crystallographic studies directed at HSA–site I drug complexes demonstrated that site I is larger than site II and that site I drugs occupy different parts of the binding pocket of subdomain IIA, even to the part adjacent to the interface with subdomain IB [6,31]. Furthermore, this site was confirmed to be a pocket comprised of two largely apolar clusters with a pair of centrally-located polar features (formed by the side-chains of Tyr150, His242, Arg257 located at the bottom of the pocket and Lys195, Lys199, Arg218 and Arg222 on an outer cluster at the pocket entrance) (Fig. 2a) [6,22]. The preference for flat aromatic compounds (as CMPF; 3-carboxy-4-methyl-5-propyl-2-furanpropionic acid) arises because they are able to fit snugly between the side-chains of Leu238 and Ala291 in the center of the cleft [6,22]. The enantiomers of warfarin bind in the same position, both involved in three hydrogen bonding interactions with Tyr150, His242, and either Lys199 or Arg222 [6,32]. Thus, site I shows poor stereoselectivity, which might also be due to the flexibility of this site.

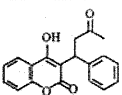
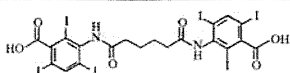
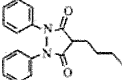
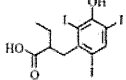
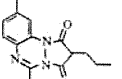
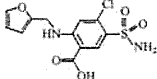
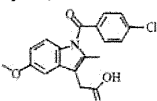
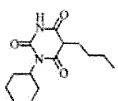
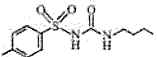
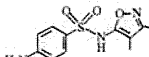
### 2.2. Site II

In addition to site I, detailed investigations have also been conducted to better understand the environment within site II. Wanwimorluck, through a quantitative structure–activity relationship (QSAR) study, suggested that site II comprised a hydrophobic cleft of about 16 Å deep and 8 Å wide with a cationic group located near the surface [33]. According to the crystal structure of HSA, site II is a largely apolar cavity with a single dominant polar patch near the pocket entrance, centered on Tyr411 and Arg410 (Fig. 2b) [13]. This arrangement of polar and apolar features is consistent with the typical structures of site II drugs, which are aromatic carboxylic acids with a negatively charged acid group at one end of the molecule that is separated by a hydrophobic center (Table 2) [3,5]. Diazepam, diflunisal, and ibuprofen, the site II drugs, interact with the hydroxyl group of Tyr411 [6]. Arg410 and Ser489 also contribute to salt-bridge formation and hydrogen-bond interactions with diflunisal and ibuprofen. Site II was proposed to be a smaller or narrower site than site I because large molecules rarely bind to site II [3,5,6,13]. Indeed, to date no one has succeeded in dividing this site in to different sub-binding regions as in the case of site I. Site II also appears to be less flexible, since ligand binding to this site often shows stereoselectivity and is strongly affected by structural modification of ligand with a relatively small group [3,5]. (*R*)-ibuprofen binds to site II with an affinity that is 2.3 times higher than the (*S*)-enantiomer [34]. Furthermore, diazepam but not its fluorinated analog flunitrazepam binds to site II [35]. Thus, although the site can bind a variety of ligands, it appears to be more restricted than site I. Meanwhile, recent crystallographic data suggest that site II can adapt to ligands



**Fig. 1.** Crystal structure of rHSA. The subdivision of rHSA into domains (I–III) and subdomains (A and B) is indicated, and the approximate locations of site I and site II are also shown. Atomic coordinates were taken from the PDB entry 1UOR. The illustration was made with PyMOL.

**Table 1**  
Typical drugs binding to site I.

Drugs (association constants)	Structures	Drugs (association constants)	Structures
Warfarin ( $3.4 \times 10^5 \text{ M}^{-1}$ ) <sup>a</sup> [26]		Iodipamide ( $9.9 \times 10^5 \text{ M}^{-1}$ ) <sup>a</sup> [26]	
Phenylbutazone ( $1.5 \times 10^6 \text{ M}^{-1}$ ) <sup>a</sup> [26]		Iophenoxic acid ( $7.7 \times 10^7 \text{ M}^{-1}$ ) <sup>a</sup> [10]	
Azapropazone ( $2.8 \times 10^5 \text{ M}^{-1}$ ) <sup>a</sup> [29]		Furosemide ( $2.0 \times 10^5 \text{ M}^{-1}$ ) <sup>b</sup> [54]	
Indomethacin ( $1.4 \times 10^6 \text{ M}^{-1}$ ) <sup>a</sup> [53]		Bucolome ( $1.5 \times 10^6 \text{ M}^{-1}$ ) <sup>b</sup> [54]	
Tolbutamide ( $4.0 \times 10^4 \text{ M}^{-1}$ ) <sup>a</sup> [10]		Sulfisoxazole ( $1.8 \times 10^5 \text{ M}^{-1}$ ) <sup>a</sup> [55]	

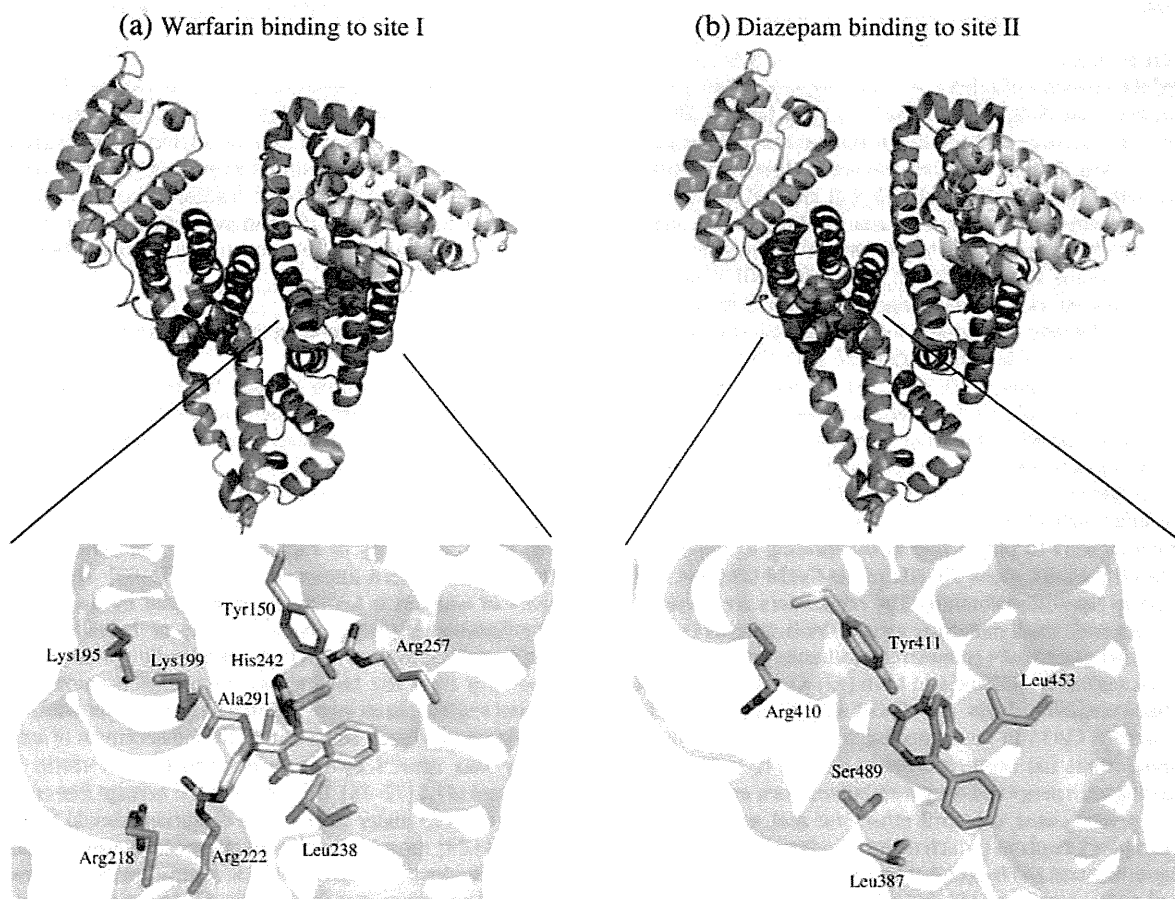
The table shows drugs that have been proposed to bind to site I with high affinity (association constant:  $K_1$ ).

<sup>a</sup> The number of high affinity of binding site ( $n_1$ ) is 1.

<sup>b</sup> Data are represented as  $n_1K_1$  in literatures.

(e.g. diazepam and long-chain fatty acid), as has been observed in site I [6]. Although there is comparatively little side-chain movement associated with site II ligand binding, the binding of diazepam, which has a

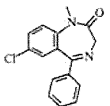
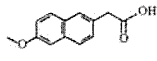
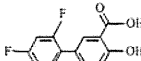
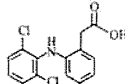
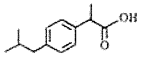
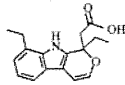
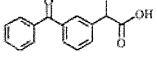
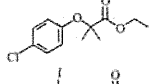
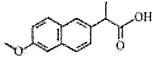
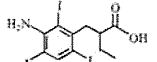
relatively large and branched structure, is accompanied by large rotations in the side-chains of Leu387 and Leu453 to accommodate the phenyl moiety of this drug [6,13,36]. Battacharya demonstrated binding



**Fig. 2.** Crystal structure of HSA complexed with warfarin (a) and diazepam (b). Drugs and amino acid residues mentioned were depicted in stick or space filling representations, and color-coded by atom-type: carbon: yellow (warfarin), orange (diazepam) or gray (residues), oxygen: red, nitrogen: blue, chlorine: green. Atomic coordinates were taken from the PDB entries 2BXD and 2BXF for warfarin and diazepam, respectively. The illustrations were made with PyMol.



**Table 2**  
Typical drugs binding to site II.

Drugs (association constants)	Structures	Drugs (association constants)	Structures
Diazepam ( $1.3 \times 10^6 \text{ M}^{-1}$ ) <sup>a</sup> [26]		6-MNA <sup>c</sup> ( $1.2 \times 10^5 \text{ M}^{-1}$ ) <sup>c</sup> [59]	
Diflunisal ( $5.3 \times 10^5 \text{ M}^{-1}$ ) <sup>b</sup> [56]		Diclofenac ( $3.8 \times 10^6 \text{ M}^{-1}$ ) <sup>c</sup> [59]	
Ibuprofen ( $3.5 \times 10^6 \text{ M}^{-1}$ ) <sup>a</sup> [26]		Etodolac ( $2.0 \times 10^5 \text{ M}^{-1}$ ) <sup>a,d</sup> [60]	
Ketoprofen ( $2.5 \times 10^6 \text{ M}^{-1}$ ) <sup>a</sup> [57]		Clofibrate ( $7.6 \times 10^5 \text{ M}^{-1}$ ) <sup>a</sup> [61]	
Naproxen ( $1.2 \times 10^6 \text{ M}^{-1}$ ) <sup>a</sup> [58]		Iopanoic acid ( $6.7 \times 10^6 \text{ M}^{-1}$ ) <sup>a</sup> [10]	

The table shows drugs that have been proposed to bind to site II with high affinity (association constant:  $K_1$ ).

<sup>a</sup> The number of high affinity of binding site ( $n_1$ ) is 1.

<sup>b</sup> The number of high affinity of binding site ( $n_1$ ) is 2.

<sup>c</sup> Data are represented as  $n_1K_1$  in literatures.

<sup>d</sup> Data is  $K_1$  for (S)-enantiomer.

<sup>e</sup> 6-methoxy-2-naphthylacetic acid, the active metabolite of nabumetone.

that subdomain IIIA can bind two molecules of long-chain fatty acid, suggesting binding flexibility exists in site II [37].

### 2.3. Other sites

Not all drugs bind to sites I or II (subdomains IIA or IIIA). Sudlow et al. suggested the existence of at least one other binding site for probenecid, amitriptyline, and debrisoquine which strongly bind to albumin [19]. Furthermore, Sjöholm [38] and Kragh-Hansen [28] demonstrated the digitoxin binding site which location has not yet been fully clarified. A crystallographic analysis by Bhattacharya et al. showed that propofol binds to both subdomains IIIA (site II) and IIIB [39]. Fusidic acid, a steroid antibiotic, binds specifically to subdomain IB, the same region as the primary binding site for bilirubin and hemin [40]. Subdomain IB was also identified as a primary binding site for lidocaine [41], and as secondary binding site for site I drugs such as azapropazone, indomethacin, iopanoic acid, triiodobenzoic acid, warfarin and AZT (3'-azide-3'-deoxythymidine) [6,16,31,32,36]. Secondary binding site for ibuprofen and diflunisal is at the interface between subdomains IIA and IIB, and that for oxyphenbutazone is in subdomain IIIB [6]. Thus, some drug binding sites different from sites I and II have been identified in subdomains that are not subdomains IIA or IIIA.

Cys34 in subdomain IA which is located in a crevice on the surface of the protein appears to play a role in the binding of some drugs to HSA. In healthy adults, about 70–80% of the Cys34 contains a free sulfhydryl group (mercaptoalbumin). The remainders are present as mixed disulfides with small molecular weight thiols, such as cysteine, homocysteine and glutathione (nonmercaptoalbumin) or are oxidized to the sulfenic, sulfinic or sulfonic acid form [42]. Covalent interaction between thiol-containing drugs and Cys34 of albumin takes place in vivo. In plasma, Cys34 in mercaptoalbumin, and probably also in nonmercaptoalbumin, has been reported to be able to participate in covalent binding with drugs and drug metabolites, such as bucillamine derivatives, D-penicillamine, captopril, ethacrynic acid, auranofin (also other gold complex), cisplatin (which mainly binds to methionine residues), nitrogen mustard and N-acetyl-p-benzoquinoneimine (a reactive metabolite of acetaminophen) [43–50]. D-penicillamine, captopril, and SA3786 (a bucillamine derivative) covalently bind to albumin in the serum of patients or healthy volunteers who are receiving these drugs [45,46,51,52]. The reactivity of these drugs in patient sera is much

higher than those found in albumin solutions [46] and in sera of healthy volunteers [52].

### 3. Clinical implications and potential applications of albumin binding

Drug binding to HSA can be affected by the presence of other drugs or endogenous compounds, or by the change of HSA structure in certain types of diseased states. As mentioned above, a change in the free fraction ( $f_p$ ) may result in altered pharmacokinetics and pharmacodynamics. It is important to evaluate the clinical therapeutic outcomes (e.g. efficacy or adverse reactions) based on albumin–drug interactions. Furthermore, safer and more efficient therapies and diagnoses using drug–albumin interactions have recently been applied in clinical stages.

#### 3.1. Displacement and drug–drug interactions in human serum albumin

Diminished plasma drug binding by the coadministered drugs is usually a result of either competitive displacement from the same binding site or allosteric displacement following microenvironmental changes at the binding site [3,5].

Historically, some drug–drug interactions have been explained based on the displacement of one drug bound to albumin by another drug, and the validity of explanations or the clinical relevance of interactions has been discussed so far [9,62–66]. The anticoagulant activity of warfarin is known to be enhanced by the coadministered anti-inflammatory drugs, phenylbutazone or bucolome [67–71]. All these drugs bind to site I with high affinities. Competitive displacement of warfarin from the binding site by phenylbutazone or bucolome occurred resulting in an increased free fraction ( $f_p$ ) for warfarin. Accordingly, it was previously believed that the enhancement of anticoagulant activity was caused by the displacement of warfarin in plasma (increment of  $f_p$ ) [72–76]. Theoretically, the average free concentration of warfarin ( $C_{ss}^f$ ) under steady state conditions should be constant in this case [9,64], meaning no obvious change in pharmacological activity should be evident. Through detailed investigations, the enhancement of anticoagulant activity was finally concluded to be mainly due to inhibition of the metabolism of warfarin, particularly the pharmacologically more active (S)-enantiomer, by cytochrome P450 2C9 (CYP2C9) [77,78]. In addition to the interaction of warfarin–phenylbutazone or

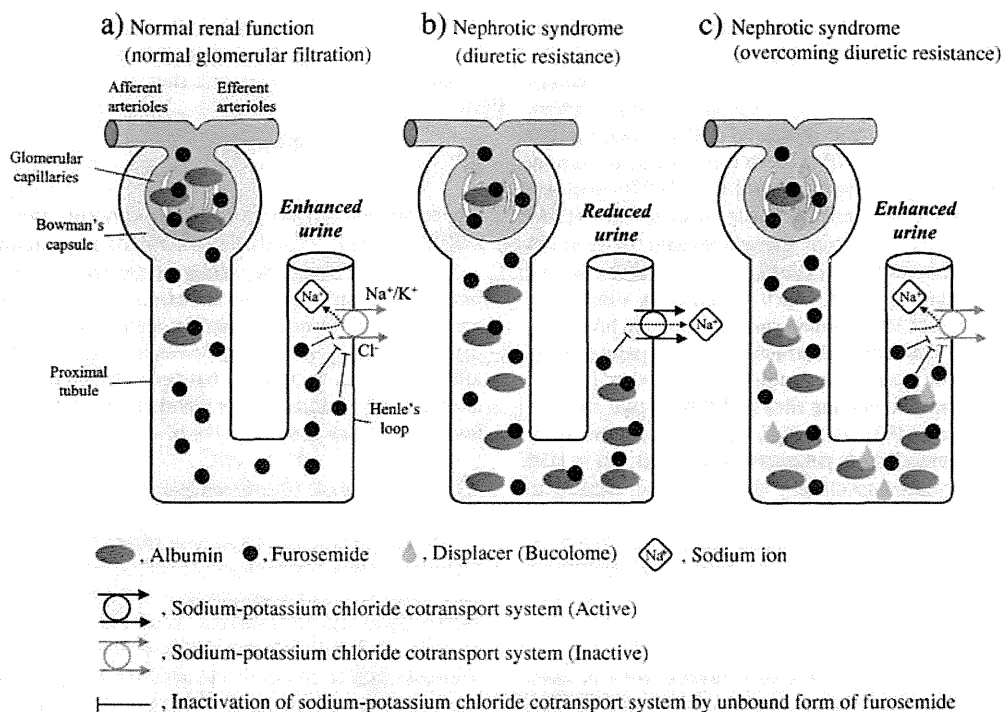


Fig. 3. Mechanism for overcoming the diuretics resistance to furosemide using drug displacement on albumin.

bucolome, the interaction between tolbutamide and sulphonamides which was also regarded to be due only to displacement, is currently explained as being mainly the result of other processes such as metabolism [79,80].

Setoguchi et al. recently reported that the pain relief in rheumatoid arthritis patients using diclofenac suppository was increased by concomitant oral administration of nabumetone [59]. Diclofenac and 6-methoxy-2-naphthylacetic acid (6-MNA; the active metabolite of nabumetone) both bind strongly to site II on HSA. Since nabumetone and 6-MNA do not inhibit CYP2C9, the rate-limiting enzyme in the metabolic clearance of diclofenac [81], they concluded that the increased pharmacological activity of the diclofenac suppository-nabumetone therapy was not due to inhibition of metabolism, but due to the transient increase in the free concentration of diclofenac. Thus, the transient change in free drug concentration due to displacement may influence the pharmacological activity of a drug in some cases. A similar observation was reported in the study on the combination therapy of flurbiprofen axetil and a lipid emulsion using a preclinical model [82].

Several attempts have been made to apply the albumin drug displacement phenomenon in achieving a particular clinical therapeutic goal [54,83,84]. An attenuated response to diuretics is frequently observed in nephrotic syndrome patients. One of the possible reasons for this diuretic resistance is albumin binding in urine. Thus, the displacement of furosemide bound to albumin was examined by Takamura et al. in an attempt to normalize the natriuretic effects of drugs in the renal tubules [54]. Bucolome was selected as a displacer drug for furosemide because of the following desirable properties: 1) it potently inhibits the binding of furosemide to albumin; 2) when administered in large doses, its plasma concentration reaches high levels; 3) it is excreted mainly in the urine; and 4) it is quite safe and suitable for repeated administration. The results obtained clearly suggest that bucolome has a potent inhibitory effect on the binding of furosemide to albumin in the urine and can partially restore the diuretic response of furosemide in patients with nephrotic syndrome by increasing the free fraction of furosemide at the site of action (Fig. 3).

Drug displacement phenomenon can also be applied in radiopharmaceutical diagnoses [83,84]. *N*-isopropyl- $p$ - $^{123}\text{I}$ -iodoamphetamine (IMP),

better suited for cerebral imaging, binds to albumin and the  $\alpha_1$ -acid glycoprotein. The displacement of IMP by concurrent amino acid infusion or 6-MNA infusion results in an increase in the free concentration of IMP, thereby causing a rapid and pronounced cerebral accumulation [83]. Furthermore,  $^{99\text{m}}\text{Tc}$ -labeled mercaptoacetylglycylglycylglycine ( $^{99\text{m}}\text{Tc}$ -MAG3), which is widely used in renal scintigraphy, is displaced from albumin by the coadministration of bucolome, resulting in rapid accumulation in the kidney and an accelerated clearance [84]. Thus, the displacement of such radiopharmaceuticals might contribute to shorter imaging times, higher signal-to-noise ratios in imaging and lower radiation doses for patients.

### 3.2. Altered drug–albumin binding in diseased states

Altered drug–albumin binding as a consequence of disease can be a result of altered albumin concentrations, structural changes in albumin molecules, and/or displacement by accumulated endogenous substances [15]. Drug binding to albumin is decreased, especially in renal and liver diseases, with a resulting increase in  $f_p$  [2,5,15]. Such an increase in  $f_p$  usually does not lead to a change in the pharmacological activity of drugs [9,64]. However, understanding the extent of change in protein binding and the mechanism can be useful in terms of setting optimal dosage regimens for patients suffering from certain diseases.

#### 3.2.1. Renal diseases

Albumin binding of drugs is decreased in patients with renal diseases such as nephrotic syndrome, chronic renal failure and uremia. In the nephrotic syndrome, the albumin concentration drops to 7–25 g/L (the normal concentration in adults;  $42.0 \pm 3.5$  g/L) [1]. An increase in the  $f_p$  of albumin binding drugs in nephrotic syndrome is known to be mainly due to hypoalbuminemia [85]. The  $f_p$  for phenytoin and clofibrate is reported to be 90 and 200% higher, respectively, in patients with nephrotic syndrome compared to normal subjects [85]. In contrast, the increased  $f_p$  in patients with chronic renal failure and uremia cannot be fully explained only by the degree of hypoalbuminemia [1]. Therefore, other factors affecting drug binding such as accumulation of endogenous inhibitors or carbamylation of albumin should be taken

into consideration [86–89]. Among these, the accumulations of endogenous inhibitors, such as uremic toxins or fatty acids, are believed to predominantly account for most of the decreased drug binding to albumin [87]. To date the binding of anionic uremic toxins such as indoxyl sulfate (IS), indole acetate (IA), hippuric acid (HA), and CMPF to albumin has been reported in human serum [90,91]. These compounds are largely responsible for the impaired binding of many drugs [91]. To elucidate the mechanism responsible for defective drug binding induced by uremic toxins, it is necessary to examine the relationship between the drug and uremic toxin-binding sites. Uremic toxins with an indole ring and HA primarily bind to site II, which is located in subdomain IIIA, whereas the location of CMPF-binding site is subdomain IIA, corresponding to site I [6,92]. Takamura et al. proposed that the reduced drug binding observed in uremic patients was due to direct and/or indirect displacements of drug from the binding sites by the increased levels of fatty acids and uremic toxins [93]. Mera et al. suggested that oxidative modification of HSA in hemodialysis patients led to alterations in HSA conformation, which decreased specifically the site II drug binding to HSA [94]. Thus, in uremia, almost all factors (altered albumin concentrations, structural change in the albumin molecules, and displacement by accumulated endogenous substances) may be involved in the altered protein bindings of drugs.

### 3.2.2. Liver diseases

In general, the rate of albumin synthesis is normal even in cases of severe liver disease [95]. Thus, other factors such as degradation and distribution between the intra- and extravascular spaces may be responsible for the reduced albumin levels associated with liver diseases (generally approximately 30 g/L) [1,95]. Decreased drug binding in liver diseases may be due to a decrease in albumin concentration, the accumulation of endogenous inhibitors (e.g. bilirubin), or changes in albumin structure. The 43% higher  $f_p$  of tiagabine in patients with moderate hepatic impairment compared with healthy subjects was proposed to be related to the lower albumin concentrations in these patients [96]. Meanwhile, the  $f_p$  of phenytoin in patients with hepatitis or cirrhosis (15.9% compared with 10.6% for control subjects) was not correlated with albumin concentration, but the concentration of plasma bilirubin [96]. Kober et al., using serum from cirrhosis patients, reported the presence of specific inhibitory effects on the drug binding to the diazepam binding site (site II) [97]. Recently, the albumin binding capacity in site II (ABiC) was clinically introduced as a convenient method for evaluating the severity of liver failure and to monitor the therapeutic effects of liver support systems (e.g. dialysis) [98]. Thus, factors affecting site II binding might play a role in the progression of liver diseases, and also decreased drug binding.

Furthermore, the effects of several diseases (e.g. diabetes, shock, acute head trauma or cancer) on drug binding to albumin have been reported [99–102]. In most cases, as mentioned above, the change in drug binding to HSA is mainly due to altered albumin concentrations, structural changes in albumin molecules, and/or displacement by accumulated endogenous substances.

A change in  $f_p$  usually does not cause a change in the pharmacological activity because if  $f_p$  were to increase, the free concentration ( $C_{ss}^f$ ) is constant in contrast to a decrease in total concentration ( $C_{ss}^t$ ) [7,16]. For therapeutic drug monitoring, therapeutic windows are usually set for  $C_{ss}^f$ , but not  $C_{ss}^t$ . Thus, the  $C_{ss}^t$  of patients ( $C_{ss}^{t'}$ ) should be translated using the following equation to confirm whether or not it is within the therapeutic window [107].

$$C_{ss}^{t''} = (C_{ss}^{t'}) \times (f_p' / f_p)$$

where  $f_p$  and  $f_p'$  are free fraction of normal subjects and patient, respectively.

$C_{ss}^{t''}$  can then be interpreted on the basis of the therapeutic window.

While it would be ideal to measure  $f_p'$ , it is not routinely available in a clinical setting. Therefore, if possible, the following alternate equation is often used [15,103,104].

$$C_{ss}^{t''} = (C_{ss}^{t'}) \times (Alb / Alb')$$

where Alb and Alb' are the albumin concentration of normal subjects and the patient, respectively. 4.4 mg/dL is normally used as Alb.

It should be noted that this equation can only be used for drugs that bind to albumin to a significant extent, when abnormal concentrations are the primary cause of binding alterations [103]. In other words, it cannot be used when drug displacing agents are present, when the affinity of drugs to proteins has been altered by coadministered drugs or endogenous substances, or when plasma proteins other than albumin bind a significant amount of the drug.

### 3.3. Extracorporeal albumin dialysis

The ligand binding property of albumin is applied to extracorporeal dialysis to remove endogenous toxins in cases of liver failure [105–112]. This method is employed to produce a more effective liver support system than the conventional hemodialysis, hemofiltration systems or charcoal hemoperfusion, because the essential toxins are water-insoluble and/or blood-bound and are therefore poorly removed by the conventional methods [108,113]. The initial clinically available systems were MARS® (Molecular Adsorbent Recirculating System) and SPAD (Single-Pass Albumin Dialysis) [113,114]. These two systems involve dialyzing blood against an albumin-containing solution (an albumin dialysate) across a highly permeable high-flux membrane. The blood-bound toxins are cleared by diffusion and taken up by the binding sites of the albumin. In MARS®, the albumin dialysate is regenerated by passage through a second dialyzer and two absorber columns (charcoal and an anion exchange columns) (Fig. 4). Another albumin dialysis method was recently made available, namely Prometheus, which is based on a Fractionated Plasma Separation and Adsorption (FPSA) system [108,113,115,116]. This system differs from MARS® and SPAD in that the patient's plasma is separated across a membrane and is then run through the adsorptive columns.

Such methods can also be used to treat drug overdose [117–122]. Drugs susceptible to these treatments generally have a narrow therapeutic range and show severe toxicity at high plasma levels, and bind to blood components. Sen et al. reported that MARS® was effective in the treatment of patients with acute renal failure and severe phenytoin toxicity, associated with cardiac arrhythmias, hepatotoxicity, and altered sensorium [119]. Serum phenytoin concentrations declined sharply, in contrast to the minor effect of the usual continuous venovenous hemodiafiltration. In addition, MARS® is effective in removing theophylline and diltiazem from overdosed patients [118,121,122]. However, application of this technique for overdosed patients is in its infancy. Further qualitative and quantitative determinations of the drug clearance by dialysis are necessary, as in the case of charcoal hemoperfusion [123,124]. Moreover, modifications of these methods also could be considered for improving the performance of the existing systems (e.g. the use of albumin mutants with increased binding affinity for bilirubin or drug [125]).

## 4. Conclusion

Drug-HSA interaction on which huge studies have been made over a long period of time is still an attractive research area not only because it is one of the key determinants of the pharmacokinetics and pharmacodynamics of therapeutic agents, but also because it has recently been applied for therapeutic and diagnostic purposes. In this review we summarized knowledge on the nature of binding sites on HSA and mechanisms of drugs binding to HSA. We also

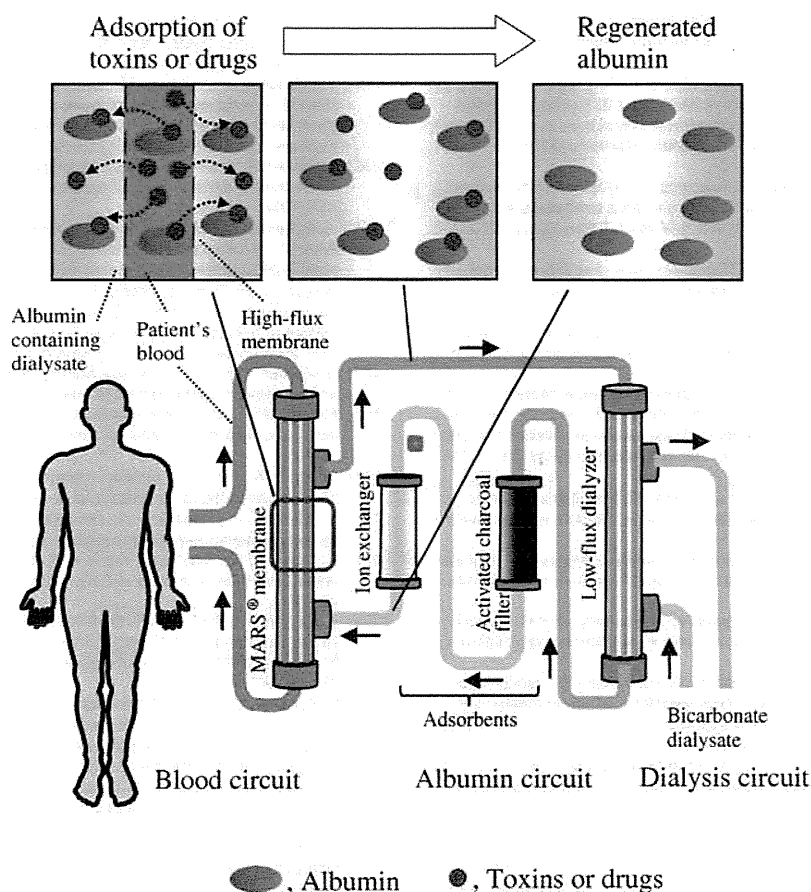


Fig. 4. Schematic drawing of MARS®.

reviewed alterations of drug binding in different diseases or in the presence of coadministered drugs. Furthermore, we reviewed the possible use of HSA in clinical applications. The information presented herein is useful in terms of providing safer and efficient therapy and diagnosis in clinical settings.

## References

- [1] T. Peters Jr., *All About Albumin: Biochemistry, Genetics, and Medical Applications*, Academic Press, San Diego, 1996.
- [2] G. Fanali, V. Trezza, M. Marino, M. Fasano, P. Ascenzi, Human serum albumin: from bench to bedside, *Mol. Aspects Med.* 33 (2012) 209–290.
- [3] U. Kragh-Hansen, V.T.G. Chuang, M. Otigiri, Practical aspects of the ligand-binding and enzymatic properties of human serum albumin, *Biol. Pharm. Bull.* 25 (2002) 695–704.
- [4] J.R. Simard, P.A. Zunszain, C.E. Ha, J.S. Yang, N.V. Bhagavan, I. Petitpas, S. Curry, J.A. Hamilton, Locating high-affinity fatty acid-binding sites on albumin by X-ray crystallography and NMR spectroscopy, *Proc. Natl. Acad. Sci. U. S. A.* 102 (2005) 17958–17963.
- [5] M. Otigiri, A molecular functional study on the interactions of drugs with plasma proteins, *Drug Metab. Pharmacokinet.* 20 (2005) 309–323.
- [6] J. Ghuman, P.A. Zunszain, I. Petitpas, A.A. Bhattacharya, M. Otigiri, S. Curry, Structural basis of the drug-binding specificity of human serum albumin, *J. Mol. Biol.* 353 (2005) 38–52.
- [7] M. Rowland, T.N. Tozer, *Clinical Pharmacokinetics and Pharmacodynamics – Concepts and Applications*, fourth ed. Lippincott Williams & Wilkins, Philadelphia, 2010.
- [8] J. Koch-Weser, E.M. Sellers, Binding of drugs to serum albumin (first of two parts), *N. Engl. J. Med.* 294 (1976) 311–316.
- [9] D.A. Smith, L. Di, E.H. Kerns, The effect of plasma protein binding on in vivo efficacy: misconceptions in drug discovery, *Nat. Rev. Drug Discov.* 9 (2010) 929–939.
- [10] J.J. Vallner, Binding of drugs by albumin and plasma protein, *J. Pharm. Sci.* 66 (1977) 447–465.
- [11] M.C. Meyer, D.E. Guttman, The binding of drugs by plasma proteins, *J. Pharm. Sci.* 57 (1968) 895–918.
- [12] W.J. Jusko, M. Gretch, Plasma and tissue protein binding of drugs in pharmacokinetics, *Drug Metab. Rev.* 5 (1976) 43–140.
- [13] S. Curry, Lessons from the crystallographic analysis of small molecule binding to human serum albumin, *Drug Metab. Pharmacokinet.* 24 (2009) 342–357.
- [14] D.C. Carter, J.X. Ho, Structure of serum albumin, *Adv. Protein Chem.* 45 (1994) 153–203.
- [15] J.J. MacKichan, Influence of protein binding and use of unbound (free) drug concentrations, in: M.E. Burton, L.M. Shaw, J.J. Schentag, W.E. Evans (Eds.), *Applied Pharmacokinetics and Pharmacodynamics: Principles of Therapeutic Drug Monitoring*, fourth ed., Lippincott Williams & Wilkins, Philadelphia, 2005, pp. 82–120.
- [16] S. Curry, H. Mandelkow, P. Brick, N. Franks, Crystal structure of human serum albumin complexed with fatty acid reveals an asymmetric distribution of binding sites, *Nat. Struct. Biol.* 5 (1998) 827–835.
- [17] S. Sugio, A. Kashima, S. Mochizuki, M. Noda, K. Kobayashi, Crystal structure of human serum albumin at 2.5 Å resolution, *Protein Eng.* 12 (1999) 439–446.
- [18] G. Sudlow, D.J. Birkett, D.N. Wade, The characterization of two specific drug binding sites on human serum albumin, *Mol. Pharmacol.* 11 (1975) 824–832.
- [19] G. Sudlow, D.J. Birkett, D.N. Wade, Further characterization of specific drug binding sites on human serum albumin, *Mol. Pharmacol.* 12 (1976) 1052–1061.
- [20] O.J. Bos, J.P. Remijn, M.J. Fischer, J. Wilting, L.H. Janssen, Location and characterization of the warfarin binding site of human serum albumin – a comparative study of two large fragments, *Biochem. Pharmacol.* 37 (1988) 3905–3909.
- [21] O.J. Bos, M.J. Fischer, J. Wilting, L.H. Janssen, Drug-binding and other physicochemical properties of a large tryptic and a large peptic fragment of human serum albumin, *Biochim. Biophys. Acta* 953 (1988) 37–47.
- [22] S. Curry, X-ray crystallography of albumin, in: M. Otigiri (Ed.), *Human Serum Albumin – New Insights on its Structural Dynamics, Functional Impacts and Pharmaceutical Applications*, Sojo University Publishing Center, Kumamoto, 2011, pp. 1–29.
- [23] K.J. Fehske, E. Jähnchen, W.E. Müller, A. Stillbauer, Azapropazone binding to human serum albumin, *Naunyn Schmiedeberg Arch. Pharmacol.* 313 (1980) 159–163.
- [24] K.J. Fehske, U. Schäfer, U. Wollert, W.E. Müller, Characterization of an important drug binding area on human serum albumin including the high-affinity binding sites of warfarin and azapropazone, *Mol. Pharmacol.* 21 (1982) 387–393.
- [25] K.J. Fehske, W.E. Müller, U. Wollert, The location of drug binding sites in human serum albumin, *Biochem. Pharmacol.* 30 (1981) 687–692.
- [26] K. Yamasaki, T. Maruyama, U. Kragh-Hansen, M. Otigiri, Characterization of site I on human serum albumin: concept about the structure of a drug binding site, *Biochim. Biophys. Acta* 1295 (1996) 147–157.